CHALMERS
UNIVERSITY OF TECHNOLOGY

Modelling the impact of groundwater leakage into subsurface structure on surface water streams

An approach using impulse response modelling for a case study at *Getå* nature reserve

Master's thesis in Hydrogeology

Markus Löfgren

DEPARTMENT OF ARCHITECHTURE AND CIVIL ENGINEERING

CHALMERS UNIVERSITY OF TECHNOLOGY

Gothenburg, Sweden 2023
www.chalmers.se

Master's Thesis 2023

ACEX30

Modelling the impact of groundwater leakage into subsurface structure on surface water streams

An approach using impulse response modelling for a case study at *Getå* nature reserve

CHALMERS

Department of Architecture and Civil Engineering

Division of Geology and Geotechnics

Engineering Geology

CHALMERS UNIVESITY OF TECHNOLOGY

Gothenburg, Sweden 2023

Modelling the impact of groundwater leakage into subsurface structure on surface water streams - An approach using impulse response modelling for a case study at Getå nature reserve

MARKUS LÖFGREN

Supervisors: Ezra Haaf, Researcher at the Division of Geology and Geotechnics,
Johanna Merisalu, Doctoral Student at the Division of Geology and Geotechnics

Examiner: Lars Rosén, Professor in the Division of Geology and Geotechnics

Master's Thesis 2023
Department of Architecture and Civil Engineering
Division of Geology and Geotechnics
Engineering Geology
Chalmers University of Technology
SE-412 96 Gothenburg
Telephone +64 31 772 1000

Cover: Getåbäcken downstream, 28th of February 2023.

Acknowledgements

At the initiation of this thesis, I had no relevant knowledge of programming languages or specific knowledge of time series analysis. Yet when I hinted about wanting to do a master's thesis with these concepts as main parts only support was given. For that, and their help throughout the project I would like to thank my supervisors Ezra Haaf and Johanna Merisalu.

I would also like to thank whoever did the manual measurements of groundwater heads in the case study are these last few years as this thesis would not be possible without preexisting datasets. Lastly, I would like to thank a resident of Getå nature reserve whom, when I had lost mine, without hesitation lent me a set of Allen keys allowing me to finish my measurements without having to return to Gothenburg or purchasing a new set.

Markus Löfgren, Gothenburg, 24-05-2023

Abstract

A hundred meters below *Getå* nature reserve outside of *Norrköping*, Sweden, a train tunnel in crystalline bedrock is planned. Due to the hydrogeological site conditions, there is a substantial risk of major groundwater leakage to the tunnel. Such a leakage may affect the nature reserve's hydrology, particularly *Getåbäcken*, a creek, which may not have its flow reduced by more than 5% due to the tunneling. This thesis aims to evaluate a data-driven modeling method to estimate groundwater drawdown due to the tunnel and investigate its impacts on the creek and its catchment area.

Pressure transducers were used to observe groundwater head change from December 2022 until May 2023. The observations indicate hydrogeological connections between glaciofluvial aquifers, fracture rock aquifers and the *Getåbäcken* after correlation analysis and baseflow separation. Impacts on the groundwater aquifers such as drawdown is therefore assumed to also impact the stream which has a baseflow index of 66%.

The observations were used to set up a groundwater time series model. Modelling presents results which indicate a clear drawdown of groundwater in the area if a leakage occurs. The results indicate that parts of *Getå* nature reserve are more resilient to recharge loss than others.

The glaciofluvial aquifer found in the center of the area is sensitive and significant groundwater drawdown is expected if a leakage into the tunnel exceeds 30 $\frac{l}{min*100m}$ whilst another, nearby, glaciofluvial deposit do not indicate a loss of aquifer recharge even at 70 $\frac{l}{min*100m}$. However, both evaluated aquifers exhibit drawdown because of the leakages.

There are indications of connections between aquifers and creek flow, along with the modelled results implying there will be significant drawdown in the area, with some locations losing groundwater recharge entirely. Thus, measures should be taken to ensure that the creek is not affected unduly by the construction of the East Link tunnel. Without measures it is likely that a leakage into the tunnel will negatively affect creek flow.

Keywords: Time Series Analysis, Impulse Response Modelling, Pastas, Transfer Function Noise Models, Groundwater drawdown, Subsurface infrastructure, Tunnelling

Table of Contents

Table of Figures

1. Introduction

In construction, all larger projects require understanding of how groundwater affects the project but also how the exploitation of the ground affects the water within it. Due to the exchange of flow between surface and groundwater bodies an impact on one may impact the other [1]. Subsurface construction specifically, does have to contend with groundwater leakage. When constructing subsurface areas, pressure loss where soil is removed leads to groundwater inflow and groundwater drainage as the leaking water is subsequently pumped away. Due to the size of these tunneling projects the volume of the leakages is substantial enough that it often may lower the groundwater level in the nearby area causing increased subsidence and negatively impacting the environment resulting in both economic and ecological damages [3].

1.1 Groundwater drawdown and surface waterways

Noted consequences of groundwater leakage are substantial drawdown [2], changes in groundwater flow patterns and changes in the groundwater chemistry [3] [4]. The consequences of leakage may also affect areas differently. An area with quicker recharge is often affected less than an area with slower recharge [4].

Groundwater drawdown is tied to further consequences such as damages to ecosystems when surface and groundwater levels decrease. By extension, the head decrease may damage vegetation and drinking water wells as they no longer reach the groundwater. It may also result in settlements and structural damages as a new force balance reaches equilibrium [5].

One specific consequence of groundwater leakage is a decrease, or in the worst-case scenario, a depletion of stream flow in gaining streams, a stream fed in large part by groundwater exfiltration [6]. In figure 1 the sequence of consequences connecting leakage to gaining stream flow is presented.

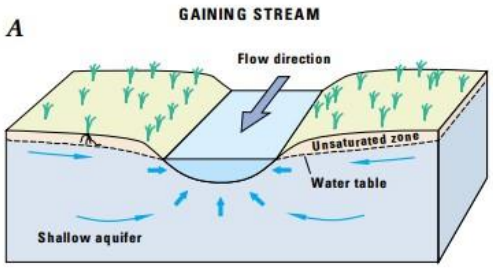

USGS, (1998), *Ground and surface water: A single source, USGS Circular, 1139*

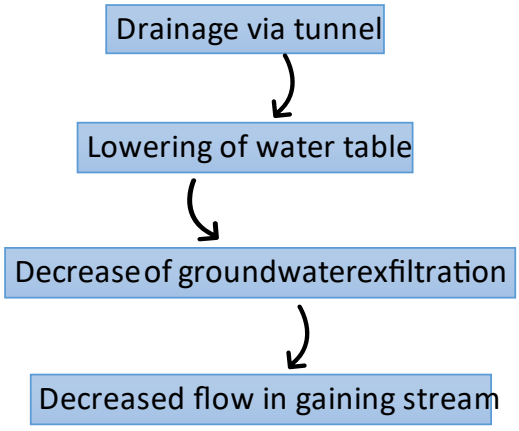

Figure 1 - Illustration of a gaining stream and a description of the potential consequences of tunnel excavation [7].

Creeks are ecosystems and hosts of life. If stream flow is depleted these habitats may disappear and the movement of nutrients stop. It has been noted that anthropogenic impacts on streams have removed habitats along streams before [8]. A depletion of these water filled areas can result in a major loss of biodiversity and in the case of wetlands release of vegetation-bound carbon dioxide [9].

1.2 Applicable methods

To lessen groundwater leakage in subsurface construction techniques such as pre grouting are used inside the tunnel. Pre grouting is specifically meant to limit inflow and control the groundwater drawdown above a tunnel [10]. However, even with such a method implemented, leakages are unavoidable. Minor leakages may be acceptable, but the risks of negative impacts are large. Therefore, along with methods to limit leakage such as pre grouting or negate its impacts by artificial infiltration, methods of forecasting groundwater changes have been created.

Manual methods such as pump tests or slug tests may be used to give an indication of aquifer properties and, by extension, ground water head changes. By extension these would also be applicable to evaluate connections to surface water. However, beyond the fact that pump tests are time-consuming, a pump test on a large scale may actively affect the surrounding environment and such a test often requires permission from relevant authorities. Modelling may therefore be used to evaluate the same parameters without unduly affecting an area. This is not saying that a model such as this is able to replace field testing. It can however be used to get an idea on how an area may respond to stress.

Existing models can be divided in to numerical and analytical models. Where numerical models require large amounts of information to create a useful description of the modelled site, analytical models are simpler regarding required data and computation [11]. Numerical models can produce very detailed results about the evaluated situation but due to the difficulty in procuring sufficient information analytical models are often used instead [11]. Such methods may include baseflow separation, impulse response modelling and time series analysis. These methods are analytical, and use gathered data and an understanding of the modelled system to achieve sufficient results.

Time series analysis is a method using data of a specific variable gathered and presented chronologically [12], the aim of which is to deduce the connection between the observed time series and surrounding stresses resulting in the time series measurements. A time series can be said to be multiple observations of the same system at different times. Time series analysis of historical data is a popular field of study in hydrogeology [13] and is useful due to its relative ease of applicability [12].

Important to keep in mind when carrying out time series analysis is the need for the time series' used in analysis to be representative of the system being evaluated. Parameters such as time series length, observation frequency and model output frequency are key when applying the models. A successful time series model calibrated against a time series dataset can be used to forecast the time series as long as input data of stresses is available.

An example of a stress applied in hydrological time series modelling is a model with the goal of modelling changes in the head of a lake. Precipitation data would then be applied as a stress on the parameter of lake head and the model would use the precipitation data and existing lake head data to calibrate itself. By extension this model would then be able to simulate the lake level solely based on stress data, in this case precipitation.

1.3 Aim and limitations

The aim of this thesis is to outline and apply a methodology to estimate the impact of groundwater drawdown on ground- and surface water using time series analysis and impulse response modelling. The modelling approach should allow forecasting of groundwater head changes due to applied stress and a way with which to tie the groundwater head change to surface water changes. The project evaluates the catchment of *Getåbäcken* in *Norrköpings* municipality, as major infrastructure exploitation is planned in the area.

The goal is to evaluate the hydrogeological connections that are present between different aquifers and surface level waterways in *Getå* Naturreservat and investigate how impacts in one part of the area may impact another as well as specifically investigate how the flow in *Getåbäcken* will be affected by the leakages into the subsurface construction.

This project is geographically contained to the *Getåbäcken* catchment area and to the use of existing groundwater wells. Whilst this project aims to evaluate the consequences of groundwater drawdown it will not evaluate solutions to the eventual drawdown. Furthermore, it will only look at the negative aspects of groundwater drawdown in relation to surface water head changes. Other consequences of drawdown will not be considered.

2. Case study area

The Swedish Transport Administration has made plans to construct a large railway section which spans most of the southeastern parts of Sweden allowing for travel between *Järna* and *Linköping* [14]. The rail is supposed to be part of the new main lines of the Swedish railway network and the project goes under the name of *Ostlänken*, or The East Link Project. The railway spans 160 kilometers and will be divided between surface rail and tunneling. Due to the many tunnels this project will create and the major differences in geological characteristics in such a large area investigation in to the tunneling effect on the environment are needed.

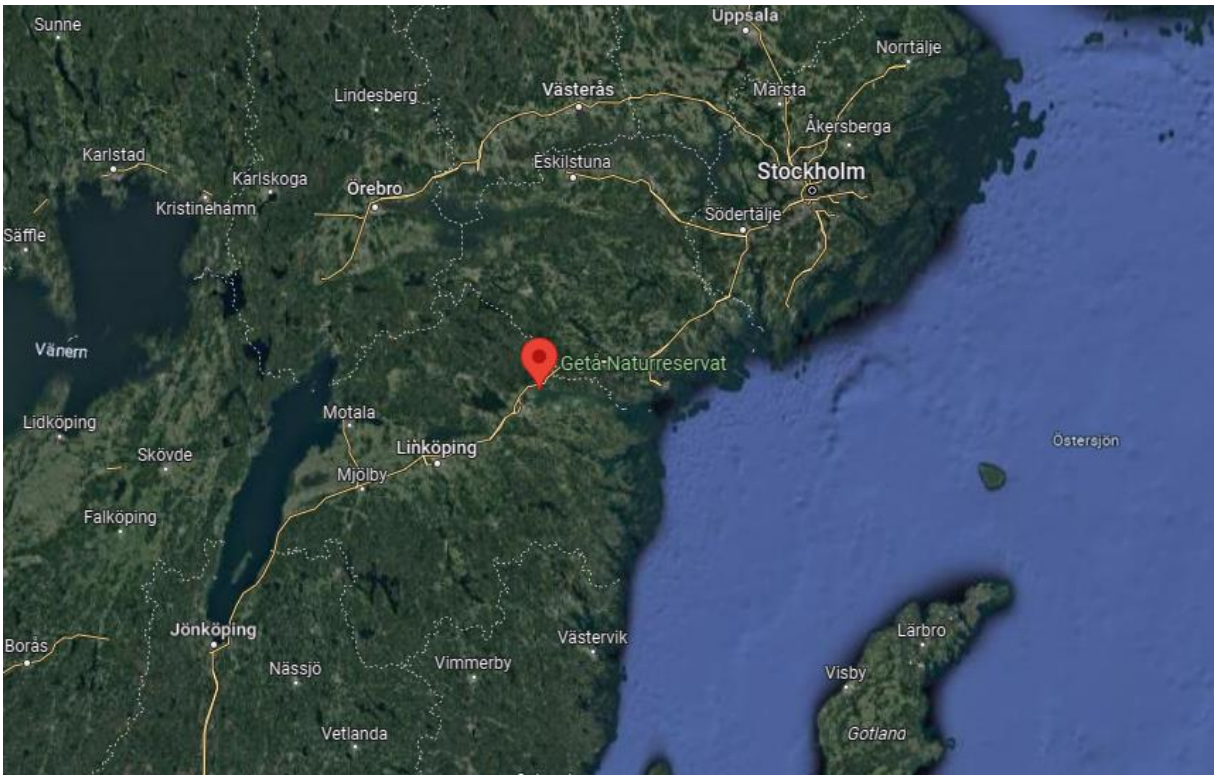

Figure 2 - Map indicating the location of *Getå* Nature Reserve in Sweden [15].

East of *Norrköping*, Sweden, *Ostlänken* will be going through a tunnel in a nature reserve area called *Getå* Nature reserve, see figure 2. The geological conditions have created a situation where there is a major risk of groundwater drawdown as, in the area, there is a large fracture zone filled with glacial material allowing for high flows, see figures 3 and 4 [16] [17]. Furthermore, in the middle of this fracture zone is the waterway *Getåbäcken*. It is a natural minor stream assumed to be fed in majority by groundwater.

The nature reserve is described as a deep ravine with a meandering stream, *Getåbäcken*, at its bottom, surrounded by old forests [18]. The larger area follows a typical east-Swedish setting regarding hydrogeology. It is a hilly area covered with thin layers of till and with valleys filled with soil such as clay or peat. Small lakes and streams cover the area ending up in *Bråviken* which is connected to the sea. The area is sparsely populated and consists mainly of forests. The main waterway in the area is *Getåbäcken*, a small, meandering stream. *Getåbäcken* is a 6 km long natural stream [19] with a natural average flow of 90 l/s [20] which achieves good ecological status. The stream is home to rare species of fish such as European river lamprey and brown trout. Around the stream, observations have been

made of common kingfishers and White-throated dippers. The vegetation found in the riverine zone is home to a wide variety of plants and species of moss [21].

Getåbäcken is of interest in the project because the tunnel will cross the stream at about 100 meters depth [22]. The geological situation and the area around the stream make it reasonable to assume that a majority of the water in the stream comes from groundwater exfiltration. This results in the streamflow being connected to groundwater levels in surrounding areas. A decrease in groundwater level because of the tunnel construction may therefore negatively impact the flow in the stream.

Due to *Getåbäckens* being declared a waterway of generally good status, a decrease in natural waterflow is limited. This is part of *Miljöbalken*, the Swedish environmental code, from 1998 where it is stated that "a municipality may not allow an activity that may harm a water environment in such a way it does not achieve its potential according to water quality assessments" [23]. For *Getåbäcken* this results in not allowing the yearly average flow to decrease by more than 5%.

2.1 The geological environment of *Getå* nature reserve

Getåbäcken has over the years eroded the area where it flows resulting in a deep ravine. This ravine is one of the main geological formations in the area. Due to the depth of the erosion, *Getåbäcken* has eroded its way down in to a glaciofluvial material which is present below the top layer of soil. The stratigraphy for *Getåravinen* specifically is assumed to be as follows, from the bottom, crystalline rock with a major fracture zone [17] followed by glaciofluvial material covered by glacial clay and sand. The glaciofluvial material can be seen on the surface in figure 3 and it is assumed that it continues below the clay throughout the ravine.

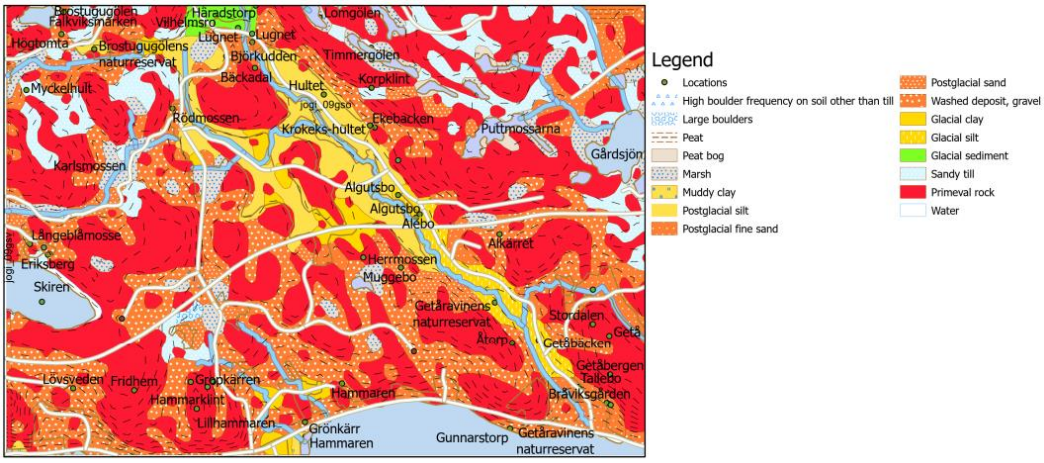

Figure 3 - Map showing surface layer soil in *Getå* Naturreservat [16]. The map was created in GIS using data from SGU and *Lantmäteriet* which was gathered from [24].

The fracture zone in the crystalline rock can be seen in figure 4. It coincides with the bottom of the ravine and creates a bedrock layer with high conductivity. Together with the glaciofluvial material, the fractured bedrock is the main aquifer in the area. The glaciofluvial is a mainly confined aquifer with unconfined areas where the material surfaces ensuring recharge to the glaciofluvial aquifer. The rock aquifer is larger than the area of *Getåravinen* and is in places covered by a layer of till which also functions as an aquifer in the surrounding areas. In the area there are also exposed sand deposits which function as unconfined aquifers as well as glaciofluviual deposits outside of the ravine itself. Due to the location of the aquifers a hydrological connection is assumed to exist between them.

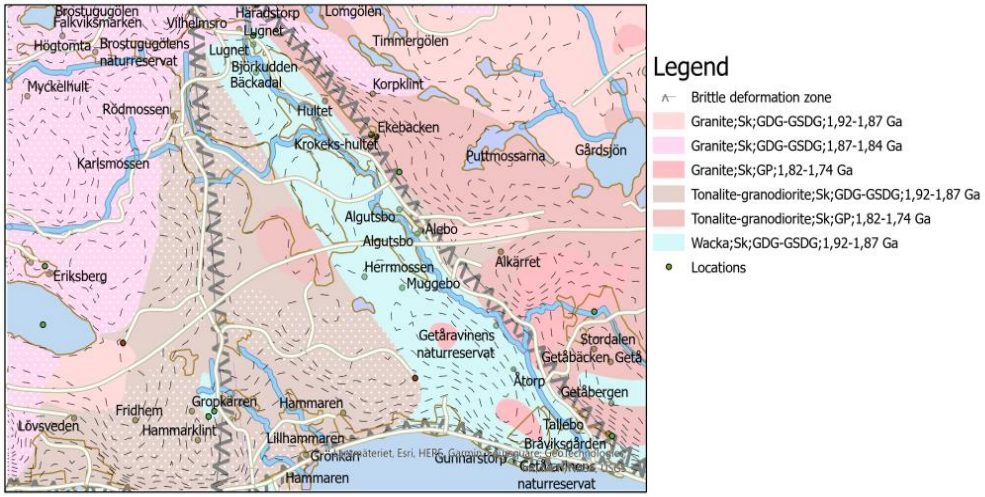

Figure 4 -Map indicating bedrock type and fracture zones in *Getå* Nature Reserve [17]. The map was created in GIS using data from SGU and *Lantmäteriet* which was gathered from [24].

Modelled soil data from The Swedish Geological Investigation, *SGU*, states that the soil depth along *Getåravinen* is between 20-30 meters [25]. Given that the stream at points in the ravine has eroded through the top layers of clay and silt and reached the glaciofluvial material the top layer is not assumed to be more than 5-10 meters thick. As the stream has eroded its way down in to the glaciofluvial material it is assumed that there is a significant hydrological connection between the stream and the confined aquifer in the glaciofluvial deposit [22]. To add to this, springs along the stream are a further indication that a portion of the water in the stream is emerging groundwater.

2.2 Site specific meteorological conditions

The meteorological conditions in *Getåravinen* Nature reserve are of interest to this report as they function as drivers for the hydrological conditions in the area. The area receives a yearly average of 665 mm precipitation according to data from the Swedish meteorological and hydrological institute, *SMHI* [26], see figure 5. The catchment area is 12.36 km^2 and contains no major water bodies, it is visualized in figure 14 [20].

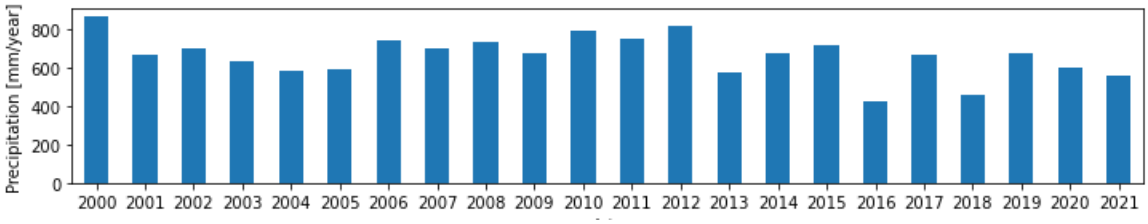

Figure 5 - Bar chart showing yearly precipitation in *Getå* Nature Reserve.

The area is almost entirely permeable with few impervious, constructed areas, being mostly forests resulting in low overland runoff flows. However, a large amount of water does not percolate and instead leave the area due to evaporation or the stream. The area is located in the zone of Sweden where *SMHI* estimates that has a yearly potential evaporation of 400 mm per year [27] and has measured the evaporation to be 450 mm the last 12 months [28]. This project will model the actual evapotranspiration in the case study area as a time series of daily evaporation is required.

The amount of precipitation which evaporates is dependent on, among other things, the temperature in the area. Data of temperature variations was retrieved from *SMHI* [29]. Figure 6 shows the mean monthly temperature in Getå Naturreservat from 2017 until 2022.

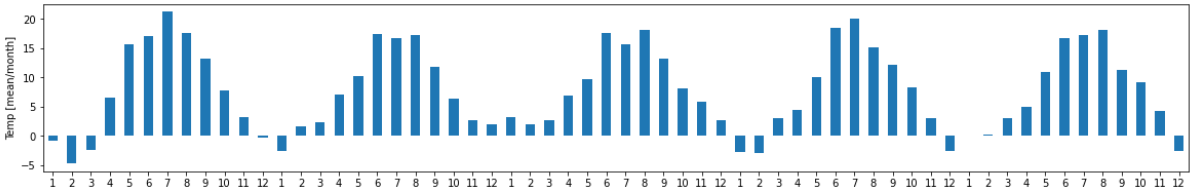

Figure 6 - Bar chart showing monthly average temperatures for some years in Getå Nature Reserve. Data was gathered over a longer time period but for reasons of clarity not all of it is presented here.

The area has a mean temperature of 7,8 degrees Celsius over the entire measured period, December 1995 until February 2023. The warmest month of the year is July which averages a temperature of 17,7 degrees Celsius. The coldest period of the year is January and February during which the average temperature is consistently below freezing. Figure 7 shows the geological and hydrogeological setting in a a conceptual model of *Getåravinen*.

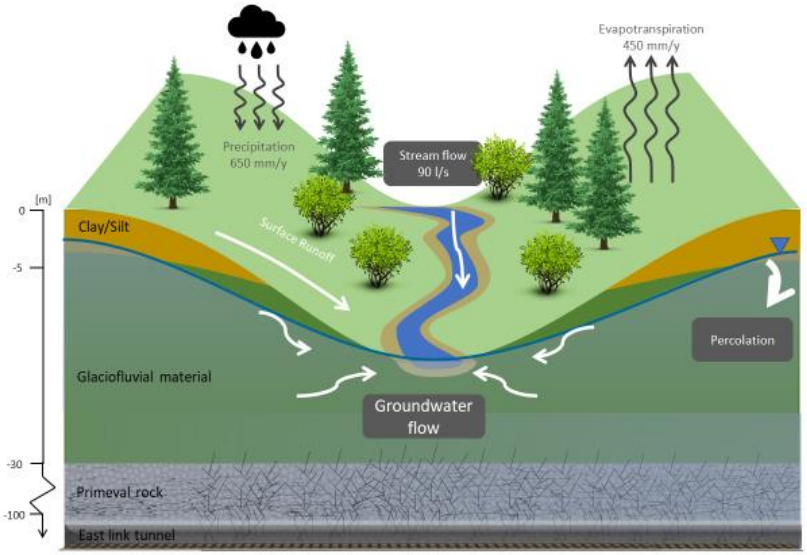

Figure 7 - Conceptual model of *Getåravinen* describing the water balance of the area.

3. Data and methods

Several modelling techniques and data evaluations are used throughout the project. The workflow of the overall project is presented in figure 8. Throughout the project, existing time series are applied to created models which evaluate evapotranspiration and groundwater head. Observed data is applied to model calibration and validation and the application of the groundwater head model is used alongside correlation analysis and baseflow separation to evaluate the results. The following chapter explains each step more in depth before presenting how application uses all the data to achieve a result.

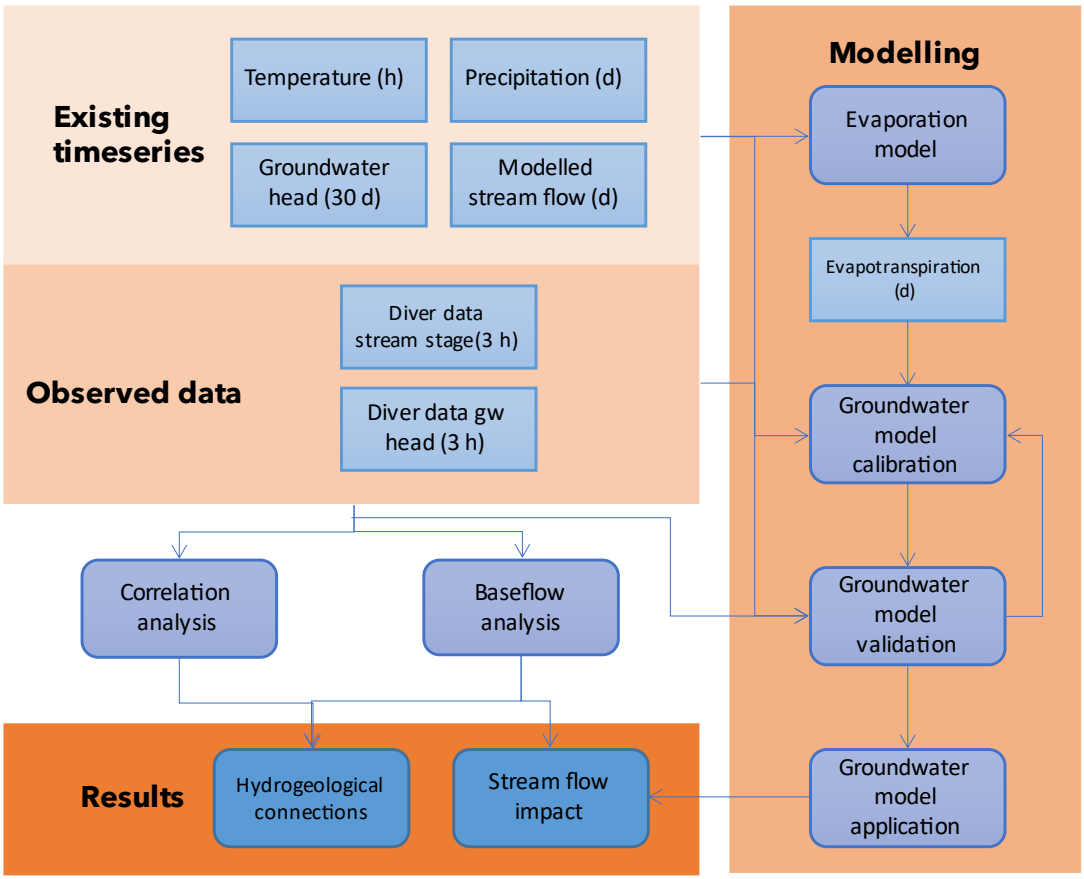

Figure 8 - Workflow for the project with frequency of datasets within brackets.

3.1 Time series data

Prior to the start of this project monthly groundwater head time series with varying lengths of time were available at a number of locations. The earlies measurements were taken in 2015 with the rest of the time series beginning later. In table 1 data of the available time series' are presented.

Table 1 - Presenting the date of the first observation and length of the time series that were available at the start of the project.

Well	Observations	First observation	Aquifer
15S113GU	80	2015-11-18	Glaciofluvial
16S113GU	70	2016-12-20	Glaciofluvial
16S115GU	69	2016-12-20	Glaciofluvial
16S116GU	69	2016-11-14	Glaciofluvial
16S117GU	68	2016-11-14	Glaciofluvial

16S130GU	65	2016-12-20	Glaciofluvial
17HB102	6	2022-06-15	Fractured rock
17HB103	8	2022-03-23	Fracture rock
17HB104	9	2022-03-23	Fracture rock

Time series data of hydrological parameters such as precipitation, temperature and stream flow were acquired from *SMHI* and updated daily. Precipitation and temperature are measured by *SMHI* whilst the stream flow in *Getåbäcken* is modelled using the lumped national hydrological model *S-HYPE* [20].

These time series datasets are going to be used together with a time series of modelled daily evapotranspiration, as input in the groundwater head change model that will be used to evaluate how the groundwater head will change. To evaluate the hydrogeological connections in the area, baseflow separation and groundwater observations will be evaluated.

3.2 Field campaign

To gather data observations absolute pressure transducer were placed in existing groundwater wells. A pressure transducer is a device that functions as a datalogger. At set intervals it takes a measurement of chosen parameters. In this case, pressure, temperature and in one case conductivity. The installation was done on two different dates due to a lack of time during the first excursion. Four transducers were installed on the 7th of December 2022 and 3 more were installed on the 22nd the same month.

Figure 9 - Picture of the well installed in *Getåbäcken*.

Of the seven total pressure transducers 6 were placed in groundwater wells and one was placed in a slitted standpipe in the center of *Getåbäcken* for measuring changes in stream stage over time, see figure 9. The standpipe was installed by pushing it in to the stream bed allowing it to stay in place despite the stream flow. The installation causes the streambed to be displaced by the tip of the portion of the standpipe and the pressure induced being installed slightly below stream bed. Stream stage measurements therefore must be corrected for the deepened streambed at the point of measurement if they are to be evaluated as stream depth.

The pressure transducers were programmed to take a measurement every three hours. Furthermore, before installing the pressure transducers a manual measurement of groundwater level in each well was done. This was done both to ensure that the transducers were placed below the groundwater level and to allow for translation of the pressure to the more conventional unit, meters above sea level, m.a.s.l.

At one of the wells a pressure transducer was installed to measure changes in barometric pressure at the same interval as pressure transducers logging groundwater and stream stage. The data from the transducer was used to compensate the measured groundwater levels to usable data. The compensation is done as the instrument measures absolute pressure, the sum of the atmospheric

pressure and the pressure of the water column above it. Given that the atmospheric pressure differs with elevation the compensation is done to simply get the value of the pressure that the water above the measurement instrument exerts. In this project all data that is presented has been barometrically compensated.

The data was compensated in the program Diver Office by Van Essen [31], the company which also manufacture the pressure transducers used in the project. The compensated data is presented as water level above the instrument. With this value it is possible to translate the data to m.a.s.l using the following equation

$$Groundwater\ head\ m.a.s.l\ [m] = Ref - MO - DO_1 + DO_n$$

Where:

- *Ref* = Reference level of the well, in m.a.s.l [m]
- *MO* = Manual observation, in meters from well head to groundwater level [m]
- DO_1 = The first Diver observation, as close to MO as possible in water level above diver [m]
- DO_n = Further Diver observations, in water level above diver [m]

Due to a lack of certainty regarding the reference level for the slitted standpipe installed in *Getåbäcken*, the data from this measurement point has not been converted into m.a.s.l and is presented as water level above the instrument. In table 2 the measurement instrument placements are presented along with necessary information to successfully compensate the data. The reference level of *Getåbäcken* an approximation of its location. Figure 10 shows a map of the area with locations of the installed pressure transducers. The colors indicating what type of aquifer the well is connected to. Well 15S113GU does not have a pressure transducer installed but is of interest to this report.

Table 2 - Presenting necessary information to convert pressure transducer measurements to m.a.s.l and to compensate the data.

Well	Installation date	GW level from top of well [m]	Reference level [m.a.s.l]
Getåbäcken	2022-12-07	---	54.6
22S107GU	2022-12-07	15.55	75.86
22S108GU	2022-12-07	12.31	75.78
16S113GU	2022-12-22	1.59	97.64
17HB102	2022-12-22	2.04	102.94
17HB103	2022-12-22	3.16	140.33
17S1KB15	2022-12-07	16.83	95.32

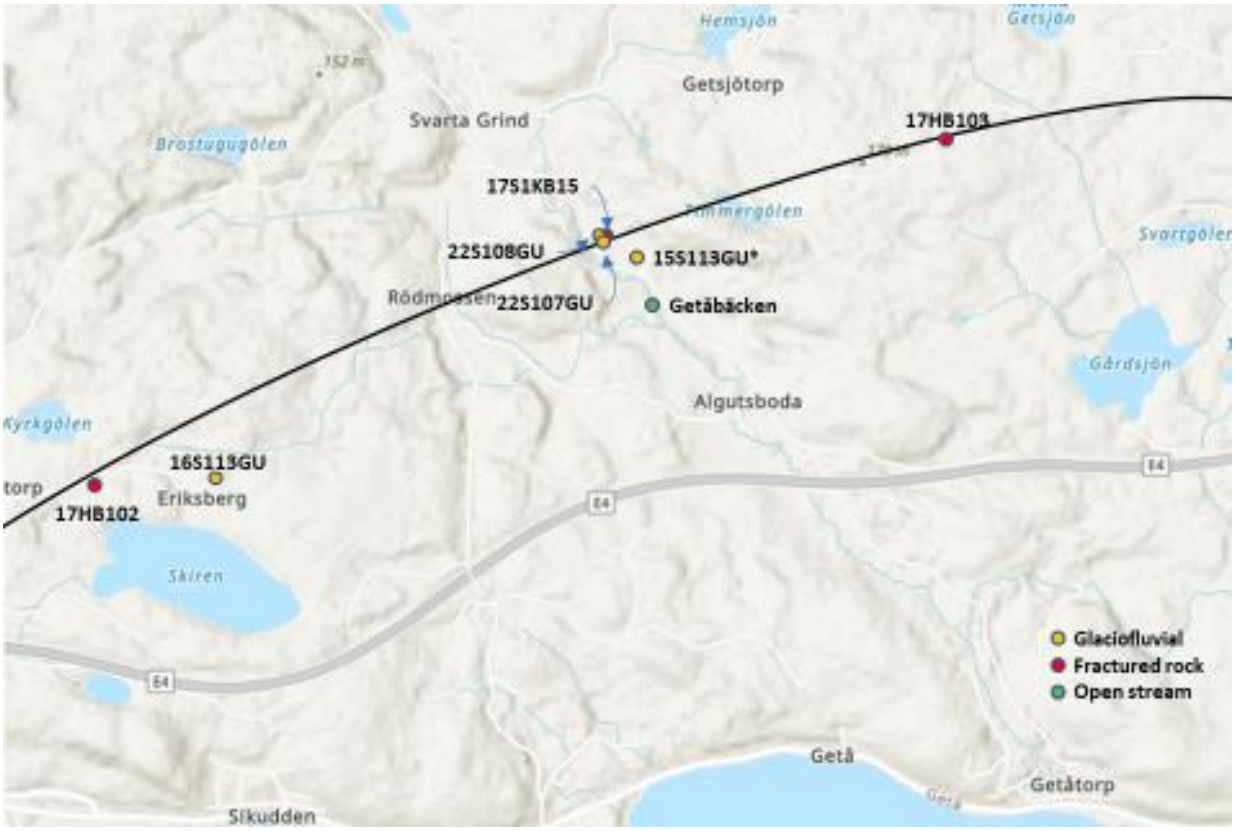

Figure 10 - Circles indicate locations of relevant wells, and a line indicating the tunnel route.

In the result chapter the range of the observation data varies due to various circumstances such as the different installation dates and that other investigations have been done in the wells which have resulted in some unusable data. For example, in figure 18 in the plot for well 22S107GU there is a period of time from 2022-12-15 and some time forward where a sharp decrease is observed. As this is not natural behavior in groundwater flow and clashes with the rest of the observations these observations were raised to be more in line with the natural fluctuations. Removing clear faulty measurements and correcting for when the pressure transducer has been moved are the only measures done on the observation datasets.

3.3 Discharge estimation in *Getåbäcken*

To estimate discharge in *Getåbäcken* tracer tests were carried out using a salt tracer [32]. The goal of the tracer tests is to determine the flow in *Getåbäcken* at different times to be able to create a function which describes the relationship between groundwater head in nearby wells and the creek flow. A successful connection between the two waterbodies would be used to evaluate the change in flow in the creek as a result of groundwater drawdown" [32].

Before starting the tracer test a specimen of water from the stream was collected in to a 5L bucket. In this bucket the background conductivity measured to 85 µS using a handheld ec-meter. Into the bucket salt was then added to increase the conductivity by 2000 µS. After 7 grams of salt was added to the bucket the conductivity measured 2080 µS. As this was occurring the streams flow was assumed to be 100 l/s. Given the assumed flow value and the 7 needed grams of salt to increase the conductivity by 2000 µS in the bucket it was concluded that 1 kg of salt was to be added to the stream to increase stream conductivity by 200 µS, the aim for a successful test.

Salt was added in a dissolved state to the middle of the stream and measurements were taken at a point about 80 meters downstream. At the measuring location the conductivity was measured using

both the handheld conductivity-meter as well as an EC-diver made by Van Essen allowing for more precise results. Measurements were done from when the salt was put into the stream until the conductivity returned to background concentrations. The gathered data was plotted over time and the integral of the conductivity over the time of the test was calculated using the trapezoidal rule. This area was the used to divide the mass of the salt inserted in the stream to achieve a calculated stream flow.

$$Stream\ flow\ [\frac{m}{s}] = \frac{Mass\ salt\ [g]}{Area\ under\ curve\ \left[g * \frac{s}{m^3}\right]}$$

3.4 Groundwater level and discharge modelling

To create the groundwater model, *Pastas* was used. *Pastas* is an open-source extension made to analyze hydrogeological time series [33]. The extension is made to work in Python which is the programming language used throughout the project. *Pastas* enables application of multiple TFN-models as wells provides simple ways to apply stresses to the models. *Pastas* was not the only Python-extension used during the project. *Baseflow* and *ETo* are two other packages used for baseflow separation and evapotranspiration respectively. The three models were used in conjunction with observed data analysis to achieve a result. How the data and modelling are applied together can be seen in figure 11.

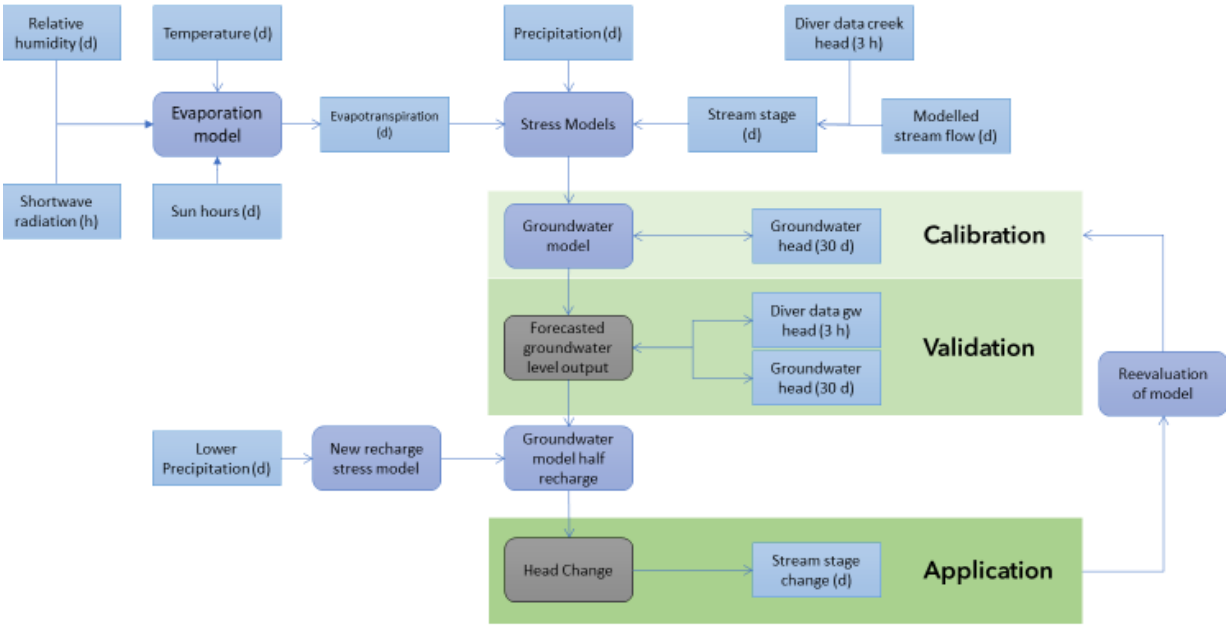

Figure 11 - Describes the workflow of the modelling process.

3.5 Baseflow separation

Baseflow separation is a method for dividing streamflow into components based on processes feeding the stream. Baseflow separation is performed in this thesis both to evaluate the connections between groundwater and *Getåbäcken* and to create a timeseries of base flow stream stage which is used in modelling. Methods are selected which separate the streamflow into quick flow, water from precipitation which contribute to stream flow shortly after such an event, and baseflow. Baseflow

can be described as water which reaches the stream after a delay [34]. This delay can for example be snow storage or groundwater storage. Baseflow is sometime referred to as “dry weather flow”.

Multiple methods of baseflow separation exist. Graphical methods wherein the low points on a hydrograph are connected by different methods or digital filter methods are two groups of methods to achieve separation [35]. This project tested multiple methods of baseflow separation using a Python extension called *Baseflow* [36]. The extension takes a flow timeseries and catchment area size as input and returns the baseflow timeseries. The baseflow separation was done on the time series of modelled flow from *SMHI* making it to reach back until 2010 and is presented on a daily scale.

The extension runs through several different methods, and then indicates what method works best based on the Kling-Gupta efficiency of the results. Kling-Gupta efficiency or KGE is a metric used to summarize model performance [37]. Traditionally the Nash-Sutcliffe Efficiency, NSE has been used but in recent years KGE has been gaining more use due to it addressing several shortcomings of the NSE. Both methods aim to express the model performance in one number. Kling Gupta Efficiency calculates the model performance using the following equation

$$KGE = \sqrt{1 - (r-1)^2 + (\alpha - 1)^2 + (\beta - 1)^2}$$

Where *r* is the linear correlation between simulated and observed values, α describes flow variability error and β is a bias term described by the equation below. In it σ is the standard deviation and μ the mean.

$$KGE = 1 - \sqrt{(r-1)^2 + (\frac{\sigma_{sim}}{\sigma_{obs}} - 1)^2 + (\frac{\mu_{sim}}{\mu_{obs}} - 1)^2}$$

The result of Kling-Gupta Efficiency varies between -∞ and 1, with 1 being a perfect match between observed and simulated. When evaluating KGE the model result is presented as a value between the two extremes. A model is preferable to use if it would be better than simply using the mean of observations. For NSE the result which indicates that the model is better than mean values is 0. Any positive NSE value indicates that the model is preferable to the mean of observations. For KGE however that value is equal to $1 - \sqrt{2} \approx -0.41$ [37]. The code for baseflow separation can be found in appendix A.

3.6 Evapotranspiration model

Evaporation was estimated based on Penman-Monteiths equation using the Python extension *ETo* [38]. The extension is provided input of temperature, sun hours, shortwave radiation, wind speed and relative humidity for each modelled day see table 3. The Penman-Monteith equation uses more parameters than that to calculate the evapotranspiration [39] but the *ETo* extension uses these datasets to estimate the rest of the required parameters based on the guidelines UN-FAO report [39]. The timeseries datasets were extracted from *SMHI*’s meterological stations. Temperature, relative humidity and wind speed were measured at the station *Kolmården-Strömsfors A* [29] [40] [41] whilst observations of sun hours and shortwave radiation were taken from the station *Norrköping Sol* [42] [43] as these datasets were not collected at *Kålmorden-Strömsfors A.*

Table 3 - Beginning of table containing input data for the evaporation model. Table has data until 2023-05-01.

date	T_max	T_min	n_sun	R_s	RH_mean	U_z
1995-12-15	1.2	-1.9	2.885000	1.28592	94.29	3.991667
1995-12-16	-0.2	-2.7	1.481667	1.15848	99.79	3.612500
1995-12-17	0.6	-3.0	5.240000	1.58508	97.50	3.395833
1995-12-18	-1.5	-8.2	1.336667	1.01916	99.59	2.863636
1995-12-19	-4.3	-9.1	3.223333	1.40148	99.04	2.600000

The output from the evaporation model is a timeseries of evapotranspiration on a daily scale during the modelled timeframe where temperature data was available. The modelled result is presented in figure 20 in the Results chapter. As evapotranspiration is inherently difficult to accurately model the results are a rough estimate of evapotranspiration from the given study period. When applied in the groundwater model the parameter *kv* in the recharge model was allowed to vary, something it does not do by default. The idea was taken from the example of snowmelt implementation in the Pastas example documentation [44]. The *kv* parameter is part of the recharge model FlexModel, which is described in the following chapter, and is vegetation coefficient which aims to explain the variation in groundwater recharge because of different types of vegetation compared to a single type of vegetation [45]. The code for the evaporation model can be found in appendix B.

3.7 Groundwater model setup and workings

3.7.1 Transfer function noise models

Transfer function noise models or TFN models are a subdiscipline of time series analysis [13] and have been shown to be successfully applicable to model groundwater head using time series data [46]. TFN models aim to use several input time series datasets, or impulses, to output a modeled series of a single parameter basically explaining the observed time series [13]. For groundwater head evaluation these impulses can be parameters such as daily precipitation, hourly evaporation or several other datasets.

A basic TFN model structure is described by Collenteur et al [13] as:

$$h(t) = \sum_{m=1}^{M} h_m(t) + d + r(t)$$

Where *h(t)* is what the model aims to simulate, which in the example is groundwater head. $h_m(t)$ is the contribution of a stress, *m*, to the head, *r(t)* are residuals and *d* is the models base elevation. The stress, *M*, is a parameter that is added to the model to indicate that the simulated result is affected by this parameter. These stresses are the impulses mentioned above. The stress' contribution to the result is calculated through the equation below:

$$h_m(t) = \int_{-\infty}^{t} S_m(\tau)\theta_m(t-\tau)d\tau$$

In the equation S_m is a time series of the stress m and Θ_m is the impulse response function associated with the stress m. Transfer function models will be used in this project. The project will also take advantage of existing impulse response functions. This will be further explained in the Method chapter.

The use of TFN models in impulse response modelling allows for modelling of complex hydrogeological systems as impulse response functions have been created for various conditions. Non-linear response functions have had an upswing during the last two decades as the previously used linear functions was shown not to be able to sufficiently model the water in the root zone [47]. Improvements such as these indicate an evolving methodology that most likely will see improvement to the precision and adaptability of the models available.

The TFN-model uses inputs of observed groundwater head, precipitation and stream stage. During the project two groundwater models were calibrated on two datasets as the response may differ withing the catchment area depending on the aquifers. Models were created and calibrated on observations in well 15S113GU, and well 16S113GU see figure 10. The datasets are plotted in figure 12. The model for 15S113GU is henceforth referred to as *Model 15GW.* The model calibrated on the time series observed in well 16S113GU will be referred to as *Model 16WL.* Both models evaluate the same parameters and use the same stresses, the only difference being the groundwater head time series used for calibration.

Well 16S113GU was chosen as a calibration well due to there being a pressure transducer installed in the well, allowing for clear validation, and the time series being sufficiently long to calibrate against. This well is also located in an area sensitive to groundwater drawdown, a wetland. Well 15S113GU does not have a pressure transducer installed but is the longest available time series and connected to a glaciofluvial aquifer where wells with pressure transducers are installed. The other wells part of this project that would be interesting to evaluate such as 17HB103 and 17HB102 have below 10 measured datapoints before this project installed instruments making their datasets insufficient to effectively calibrate the model on.

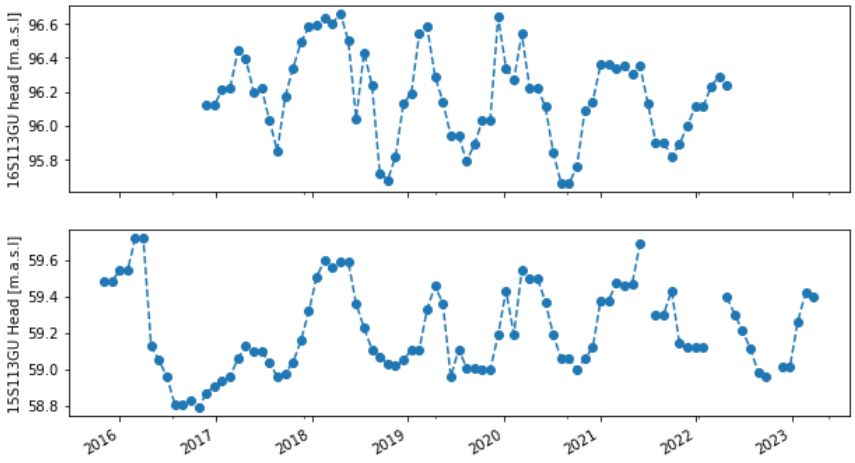

Figure 12 - Time series of groundwater head. These series are used for model calibration.

3.7.2 Recharge and stress models

Two stress models that were used in this project and they apply the stresses of stream stage and groundwater recharge. Throughout the project multiple combinations of recharge models and impulse functions were evaluated. Applicable models show good results for multiple combinations.

In the end however the most optimized model was found using the settings presented in the following parts of the report.

Both *Model 15GW* and Model 16WL use the FlexModel recharge model. FlexModel was created by Collenteur et al in 2021 [45]. FlexModel is, according to the authors based on the FLEX conceptual modelling system used in stormwater modelling. FlexModel simulates a soil-water storage concept to simulate the root zone storage of water. It conceptualizes a system as two connecter reservoirs, see figure 13.

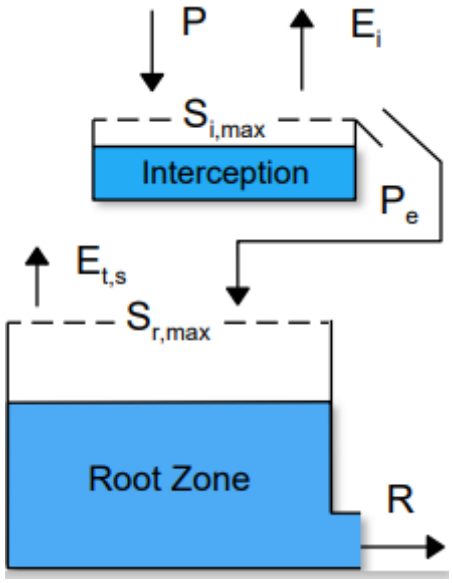

Figure 13 - Conceptual model for FlexModel [45].

The model takes precipitation and fills the interception basin until capacity is exceeded. In this conceptual reservoir water can evaporate which introduces nonlinearity to the groundwater recharge. Further information regarding the model creation can be found in "*Estimation of groundwater recharge from groundwater levels using nonlinear transfer function noise models and comparison to lysimeter data"* [45].

Both the recharge models and the stress models apply response functions which govern the response of the dependent variable, in this case groundwater head, to an independent variable such as precipitation [48]. In this project all recharge models and the stress model use the Gamma response function which is widely applied and very versatile when investigating hydrological response [48]. This stress model uses precipitation and evaporation data to simulate the effect of these parameters on the groundwater head.

Together with the recharge model, a stress model which applies a stress in the form of *Getåbäckens* stream stage is added to the groundwater model. As the stream and the groundwater is assumed to have a significant connection, patterns noticed in the stream head is expected to be emulated in the groundwater levels. This assumption is only possible as long as the stream is gaining. The assumption of a gaining stream is evaluated via the baseflow separation but it is strengthened by the fact that there are no major waterbodies in the catchment area, see figure 14. This indicates most water in the stream is either groundwater or precipitation. The stress model representing Getåbäcken uses stream stage as input and uses the Gamma response model for both aquifer types.

Figure 14 - Catchment area for *Getåbäcken* [20]. No major waterbodies allow for the assumption that most of the water in the stream comes from groundwater. The orange dots indicate well 16S113GU and well 15S113GU.

At the start of the project a timeseries of stream stage was unavailable. The project therefore installed a pressure transducer in *Getåbäcken* to observe the stream stage. The observations were then correlated against the modelled data from *SMHI*'s HYPE-model. A high correlation allows for translations of modelled flow to stream stage via an exponential trendline, creating a time series of stream stage going back to when the HYPE-model was initiated in 2010.

3.7.3 Noise model

The recharge and stress models are applied to the groundwater time series model together with a noise model. As a modelled system will never completely match a set of observed datapoints the difference in the observed and simulated timeseries can be used to create a timeseries of its own. This timeseries is usually called a residual timeseries. The residuals, the difference, occur due to errors such as modelling parameters, simplifications or errors with observations to name a few [49].

A model residual at a timestep is often correlated with an earlier timestep observation. Modelling the residual timeseries can have several purposes among which is predicting residuals at unobserved timesteps. This allows for optimal use of model prediction and observations which increases the total model accuracy [49]. The model of the residual time series is called the noise model. The noise model is a vital part of the transfer function noise models and is provided via *Pastas*. This project uses a standard noise based on *Modelling irregularly spaced residual series as a continuous stochastic process* [49].

3.8 Application of the groundwater model and scenario simulation

When calibrating the model, the mentioned stress models take input of the time series of precipitation, stream stage and evaporation. The datasets of precipitation, temperature and evaporation have data spanning back until 1995. Whilst stream stage only spans back to 2010. Calibration ran from the start of the dataset until 2022-09 after which validation will begin. Three settings will be used when calibrating Model 15GW and Model 16WL. The difference between the three settings is the dataset used in the stream stage stress model. In table 4 the different settings are presented.

Table 4 - The tested calibration settings

Well	*Stream stage data used.*
15S113GU	Observed stream stage
	Baseflow stream stage
	No stream stage stress model
16S113GU	Observed stream stage
	Baseflow stream stage
	No stream stage stress model

Calibration is done from the start of the datasets until 2022-09. As calibration completes the model was used to simulate the groundwater change from 2022-10 until 2023-05.

Evaluation is carried out on the coefficient of determination, R^2, which indicates the proportion of the variance in the dependent variable that can be explained by the independent variable [50]. Generally, it can be considered a goodness of fit variable where a high value indicates that the model is a good fit for the provided data. Along with the coefficient of determination the root mean square error (RMSE) and the Akaike Information Criteria (AIC) will be presented. The RMSE indicates model accuracy and allows comparison between similar models. As RMSE is scale dependent the main use is in comparing models using similar variables [51]. The AICs goal is similar, it is a value which helps comparing different models. The AIC will not indicate how good a model is, simply indicate which of a set of models is the best [52].

The model which shows the best performance was then used in model application to evaluate different leakage rates into the East Link tunnel. The different recharge scenarios were simulated by a decrease in precipitation. The leakage amounts were arbitrarily chosen and are not representative of any expected leaks. Applying the leakage scenarios was done by having the model calibrate on datasets which does not differ during the period of calibration. However, from the 1st of October 2022, the month after calibration concludes, the precipitation dataset will begin to differentiate for the 3 scenarios. A fraction of the precipitation relative to the leakage rate evaluated will be removed from that point until the end of the simulation.

The fraction of precipitation removed was calculated based on the fact that 212 days pass between 01-10-2022 and 01-05-2023 during the catchment area, which is 12 300 000 m^2, received 389 mm precipitation. As the tunnel spans 4 km within the catchment area and an assumption was made to use 70% of the area to calculate the total precipitation. This was done to take precipitation falling and not reaching the tunnel and the precipitation leaving via overland waterflows into account. Total precipitation was then compared to the different leakage scenarios, see table 5.

Table 5 - Leakage scenarios

Leak per 100 m	30	70	**[l/min]**
Leak within catchment	1200	2800	**[l/min]**
Total leak within area	6912000	16128000	**[m3]**
Fraction of precip	21.13%	49.29%	**[-]**

The leakage rates were, as stated, arbitrarily chosen to evaluate the response. Once a tunnel is constructed measures are usually taken to inhibit leakage into the excavation. This results in, if measures are successful, the leakages being significantly lower than the ones investigated in this report. However, as this project simply aims to evaluate the effect of leakages on the groundwater head in the area it assumes no measures have been taken before tunneling beings. As such, the

chosen rates are a large fraction of the recharge in the area over the modelled time period. The code for the groundwater model is found in appendix C.

4. Results

This chapter presents the results from the different evaluations done throughout the project. It begins by presenting the result specifically tied to *Getåbäcken* such as discharge estimation, baseflow separation and stream stage time series. It then presents the observed groundwater head fluctuations before concluding by presenting the results of the groundwater head model.

4.1 Discharge estimation

Tracer tests were carried out 6 times at three different dates for different flow conditions, see table 7, appendix D. One of the tests on 2023-03-06 was negatively affected by the creek being frozen and was therefore disregarded. Figure 15 the tracer breakthrough curve from each occasion when tests were done is presented.

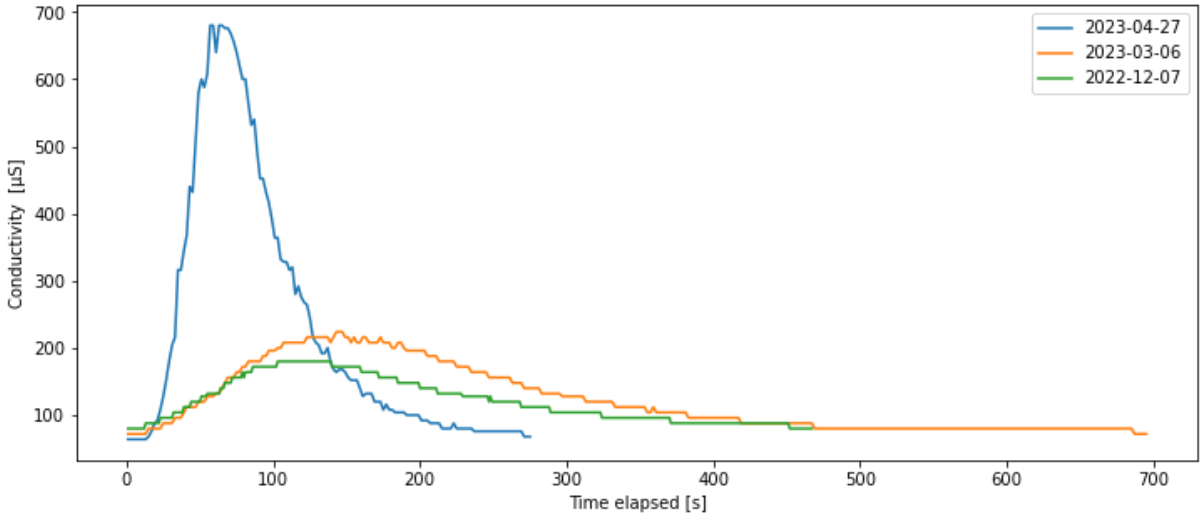

Figure 15 - Plots of tracer results

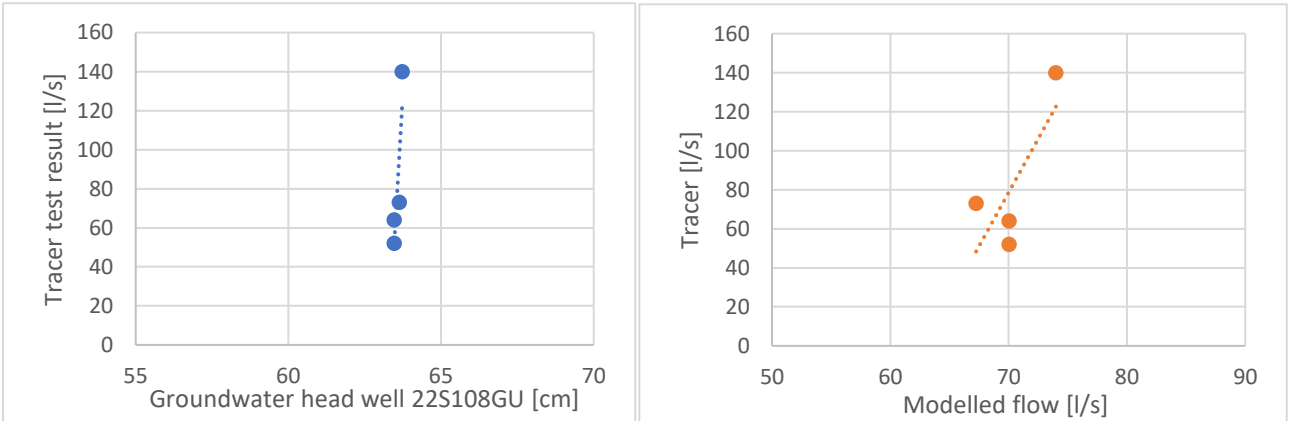

Figure 16 - Presents the results of the discharge estimation plotted against groundwater head and modelled flow.

Given that the dataset is so small the uncertainties tied to this method are deemed too large to allow conclusions to be drawn from the data. The method itself is sufficient to be applied to describe the relationship between groundwater head and stream flow but it requires more datapoints before it is applicable. The fitted trendlines in figure 16 does not indicate a reasonable relationship but may, with more observations be more applicable. The same situation is seen when plotting the tracer tests against the modelled flow in figure 16.

4.2 Baseflow separation results

For the input time series, the *Baseflow* extension indicated that Boughton method was the preferred method to use on the dataset, having the highest KGE-value among the methods the extension tests (0.76). The optimal method and its parameters can vary depending on the input dataset and the conditions found at the observation site [53]. Boughtons method is a digital filter method using two parameters. It works by applying a low pass filter to a hydrograph where the parameters of the filter are estimated so that baseflow does not exceed the hydrograph [54]. More information on the method can be found in [55].

With the baseflow separation done the baseflow index (BFI) of the stream was calculated by first calculating the fraction of the flow at every timestep that is made up of baseflow. During only baseflow this fraction is 100%. Averaging these fractions for each observed timestep gives the BFI and an indication on how tightly connected the stream flow is to surrounding delay structures.

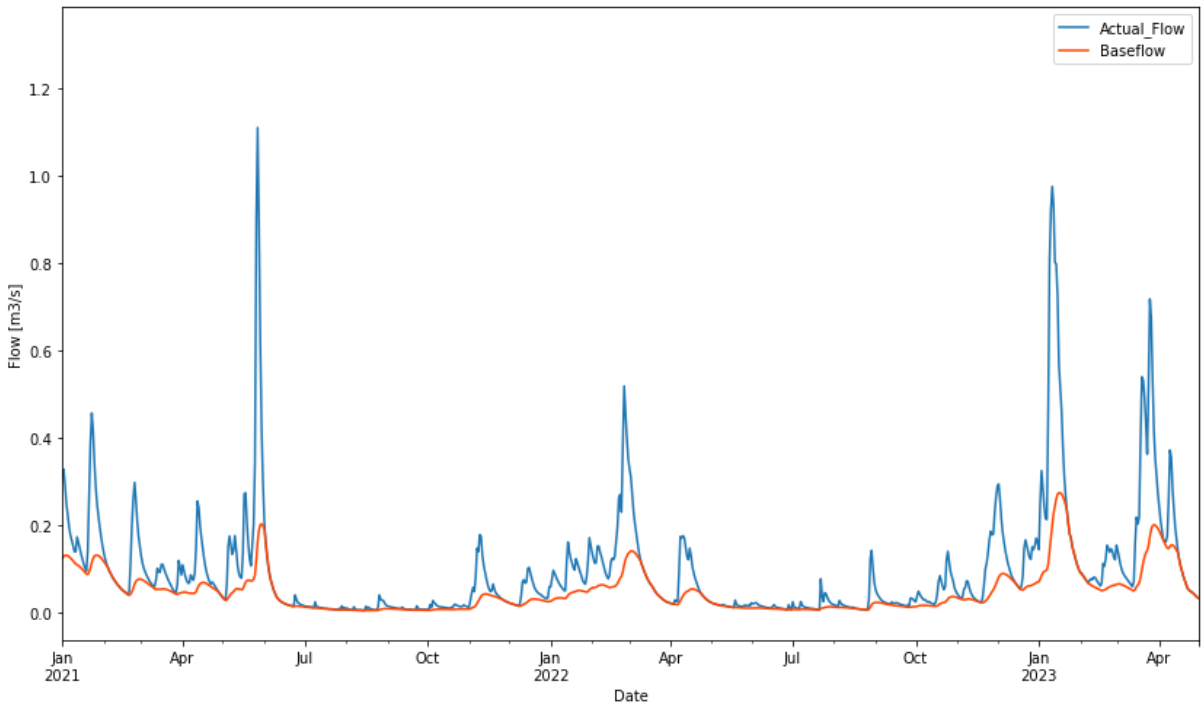

Figure 17 - Results of the baseflow separation.

Figure 17 shows that the baseflow follows the actual flows pattern of fluctuation in flow but disregards the shorter peaks. It is expected as the baseflow is not as affected by precipitation events that the actual flow is. From this dataset the baseflow separation index for *Getåbäcken* was calculated. The resulting BSI was 0.66 indicating that 66% of the water in the creek is delayed flow from, for example, groundwater, snow storage or other delay mechanisms.

The baseflow separation strengthen the assumption that *Getåbäcken* is a gaining stream. With 66% of the flow being baseflow the connection to the stream flow from the surrounding groundwater aquifers are substantial. From the plot in figure 17 it is also clear that the baseflow ignores large parts of the quickflow and only increases when the flow spends a longer period on an elevated level. In the same figure can also be seen that the creek has regular increases in flow during the winter which indicates that snow storage is not a large factor in the delay precipitation reaching the stream, confirming the information from *SMHI*.

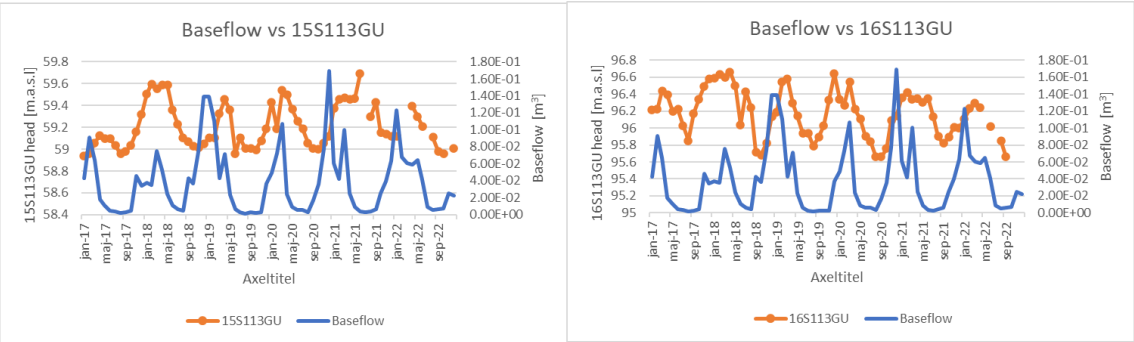

Figure 18 - Comparison between modelled baseflow and calibration time series'.

The lowest flows occur without fail during the summers. Evaluating the plotted baseflow compared to the low frequency datasets in figure 18 seasonality of the baseflow can be seen. Comparing the groundwater fluctuations with the baseflow fluctuations show indications of baseflow being tied to groundwater recharge of the previous year which was expected and explains the lack of flow in the summer when recharge is at its lowest and the consistent increase during fall when recharge peaks.

However, even with the baseflow separation indicating baseflow a major part of the stream flow there isn't complete certainty around the stream being gaining throughout the year. As the groundwater exfiltration in to streams isn't a linear relationship [56] and there may be times in a given year when the stream is not gaining but losing instead, where water infiltrates through the creek bed to groundwater [6]. Even so, over a time period of a year the assumption that the creek is driven in large part by baseflow stands.

4.3 Pressure transducer observations

In figure 19 the well heads for each well is shown for the entirety of the study period. The occasions at which data were collected are only of interest for the tracer tests and has no vital role in the evaluation of the other timeseries. Unfortunately, when collecting data on the 6th of March it was noted that data from the instrument placed in well 17S1KB15, connected to the fracture aquifer, was unusable due to complications with its installation. Therefore, data from this well is missing for the first part of the study period.

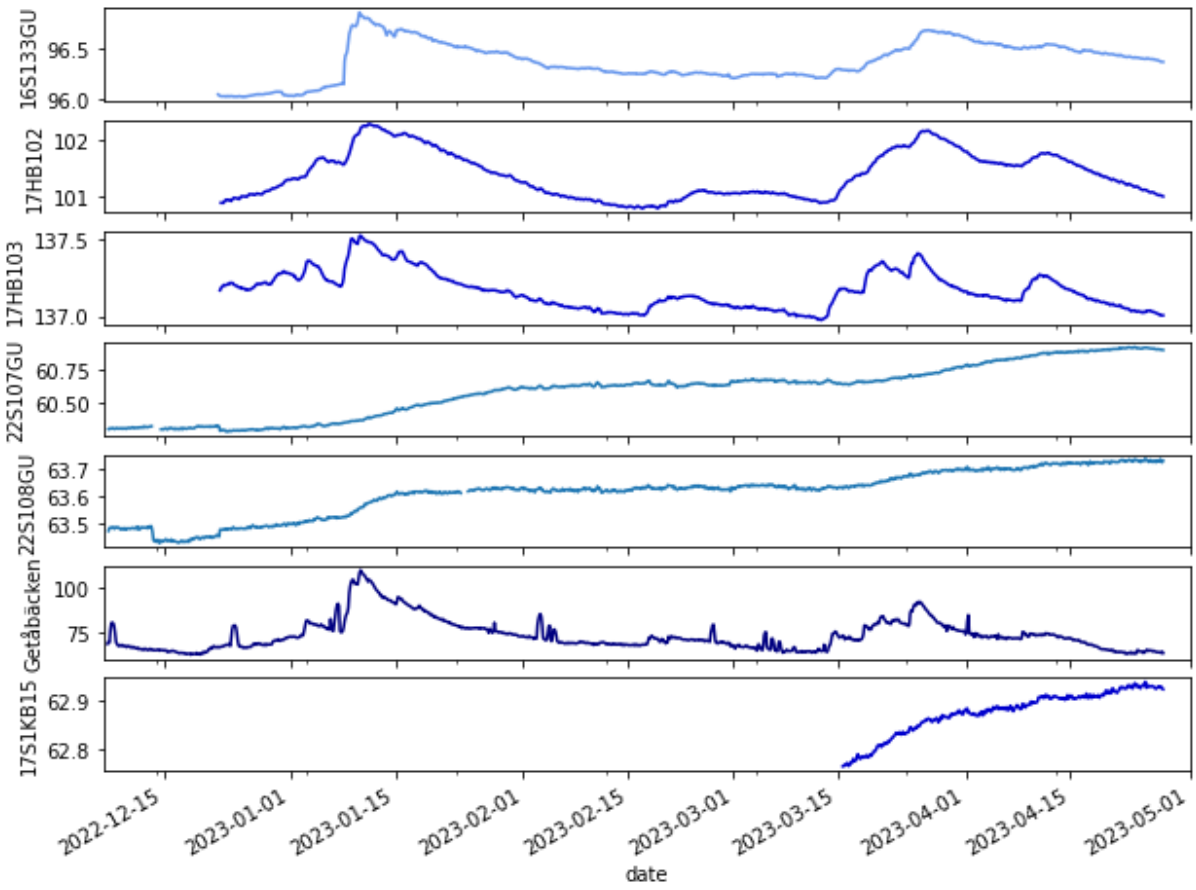

Figure 19 - Plotted time series data from pressure transducer measurements

Well 16S113GU is located in a wetland and connected to an assumed confined glacoifluvial aquifer. Wells 17HB102 and 17HB103 connect to the wetland aquifer. Wells 22S107GU and 22S108GU connect to the confined glacifluvial aquifer located in the middle of the catchment area. The difference in color simply indicate that the wells are connected to, or exist in similar environments.

In the observed data, clear similarities in the patterns of groundwater fluctuation between the different wells can be seen. Throughout *Getå* Nature Reserve clear increases of groundwater head is observed, in both the fracture aquifer wells and well 16S113GU a quick response to a recharge event initiated by a few days of precipitation is seen, precipitation for the observation period is presented in appendix E. At the same time a recharge initiates in the glaciofluvial wells 22S107GU and 22S108GU however at a slower pace. All recharge events identified in figure 19 for the different wells have clear origins in the precipitation events seen in appendix E indicating that aquifer recharge isn't delayed rather it happens rapidly after a precipitation event takes place.

It is reasonable that the rock aquifer would have a similar response throughout the area. However, the speed of the response is worth noting. A quick response to the recharge event is clearly indicated in the fracture rock aquifer. This pattern is also seen in *Getåbäcken* as well as 16S113GU indicating that there may be strong connections between the rock fracture aquifer, the creek and the glaciofluvial aquifer deposit connected to 16S113GU.

Correlations between the datasets were evaluated to further understand how the different aquifers are connected. The correlation was done using Spearman method ranking the observations and in table 6 the correlation coefficient for the available data is presented.

Table 6 - Correlation between measured data for all wells

	Baseflow	17HB102	17HB103	16S113GU	22S107GU	22S108GU	17S1KB15	Getåbäcken
Baseflow	-	0.91	0.79	0.77	-0.05	-0.01	-0.54	0.79
17HB102	0.91	-	0.79	0.77	0.07	0.12	-0.60	0.76
17HB103	0.79	0.79	-	0.43	-0.40	-0.32	-0.76	0.84
16S113GU	0.77	0.77	0.43	-	0.35	0.37	-0.15	0.57
22S107GU	-0.05	0.07	-0.40	0.35	-	0.98	0.97	-0.32
22S108GU	-0.01	0.12	-0.32	0.37	0.98	-	0.99	-0.27
17S1KB15	-0.54	-0.60	-0.76	-0.15	0.97	0.99	-	-0.82
Getåbäcken	0.79	0.76	0.84	0.57	-0.32	-0.27	-0.82	-

The indications of hydrological connections are strengthened by the correlation analysis in table 6. The correlation between 17HB102 and 17HB103 is, as expected, high at 0.79. Noteworthy is the high correlation from the rock aquifer wells to other observations points in the area such as 16S113GU which has a 0.77 correlation coefficient with 17HB102 and *Getåbäcken* which has high correlations with both fracture aquifer wells, 0.76 and 0.84 for 17HB102 and 17HB103 respectively. Just as the actual flow in *Getåbäcken* the baseflow has high correlation with the indicated wells. All in all, it paints a picture of quick responses throughout the groundwater aquifers as well as the surface water bodies in the area. Especially as a similar response identified because of a recharge event in the middle of March and in the middle of April.

This pattern is however not noticed in the glaciofluvial aquifer below wells 22S108GU and 22S107GU. In the observation time series for these two wells the recharge events are clearly indicated by an initiation of a slow groundwater head increase. In figure 19 its observed that the runoff from the aquifers occur at different rates. Wells 22S107GU and 22S108GU has a slow increase in groundwater head after a recharge event takes place whilst the others wells exhibit a decrease back towards pre-recharge levels. This indicates a difference in runoff rates and a lack of connection between these groups of aquifers. Similairy, the quick responses seen in the groundwater levels throughout the Nature Reserve and in *Getåbäckens* baseflow indicates that there may be a hydrological connection between these aquifers and the creek. This means that the groundwater drawdown found during model application would have an apparent impact on the flow in *Getåbäcken*.

As the correlations between the different aquifers differ depending on what specific well is being evaluated it may be that high correlations depend on other things than direct hydrological connections. As 16S113GU has a higher correlation to 17HB102 than 17HB103 it may be that the connections are tied to geographical distance. All the wells may also simply have quick responses to precipitation which would drive the correlations as they all quickly rise once precipitation occurs. However, the fact that they decrease at similar rates through large parts of the catchment area indicate that there may be connections between the aquifers as if the decrease instead occurred from several unconnected aquifers the rates would be more varied.

However, even though the quick responses in many wells strengthen the connections uncertainty still exists as the time of observation only spans a few months. To properly evaluate seasonality and validate these models a longer time period should be observed to properly see the response to all types of stress event. Unfortunately, the low frequency of the older time series make them unsuitable for this evaluation due to the fact that quick changes are observed by the pressure transducers. For example, the entirety of the peak occurring in January occurs and returns to pre-peak levels over the span of 20 days meaning that a 30-day frequency dataset may miss it entirely.

4.4 Creating a stream stage timeseries

A correlation analysis of the observed daily average creek head and the modelled creek flow by S-HYPE from *SMHI* resulted in a correlation coefficient of 0.92, calculated using Pearson. The high correlation indicates a clear relationship, see figure 20.

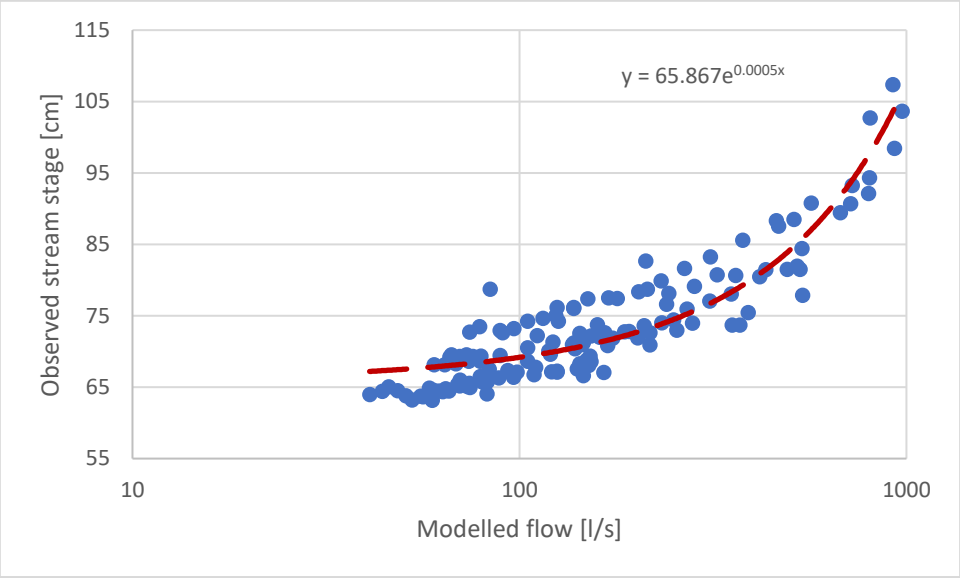

Figure 20 - Correlation and trendline of measured head versus *SMHI* modelled flow.

The equation of the exponential trendline that was fitted to the dataset was then used to calculate the stream stage for the entire timeline that S-HYPE has been active resulting in the stream stage time series presented in figure 21.

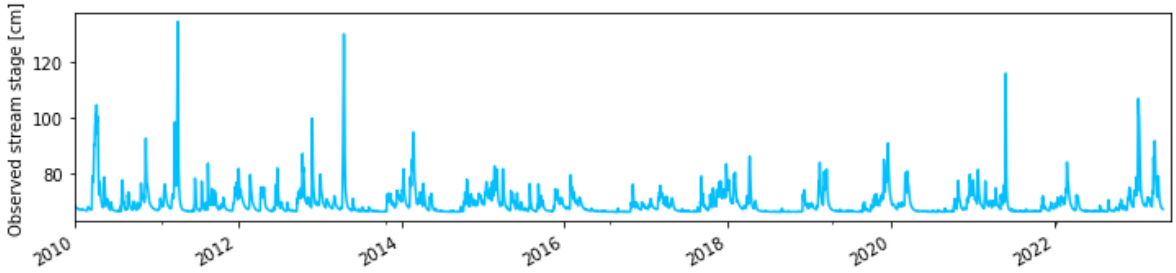

Figure 21 - Time series of *Getåbäcken* head after conversion from *SMHI* modelled flow.

4.5 Evapotranspiration model output

The figure below presents the output of the evapotranspiration model in the form of a plotted timeseries. The model produces a timeseries of daily evapotranspiration in the evaluated area.

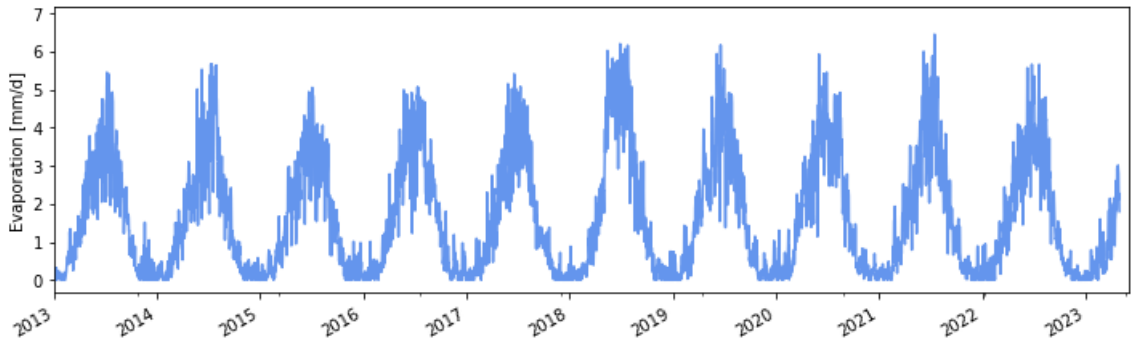

Figure 22 - Time series of evapotranspiration in *Getå* Nature Reserve for the last 10 years.

The modelled evapotranspiration is on a yearly average higher than the values that *SMHI* presents for the area. With an average yearly evapotranspiration of 584 mm, it exceeds SMHI's values by about 20%, being measured at 450 during the last 12 months, but is still deemed applicable in this project. In figure 22 its clear that the evapotranspiration peaks around July which is expected as it is the warmest month of the year in the area. Figure 22 presents the total yearly evaporation according to the model.

4.6 Model calibration and validation

Along with the calibration time series of observed heads both models take input of the parameter time series' shown in appendix F. These are used as input in recharge models and are necessary to use the model for forecasting. The results of model calibration are presented below along with the observation time series and the coefficient of determination. Fit reports for all presented models are found in appendices G and H.

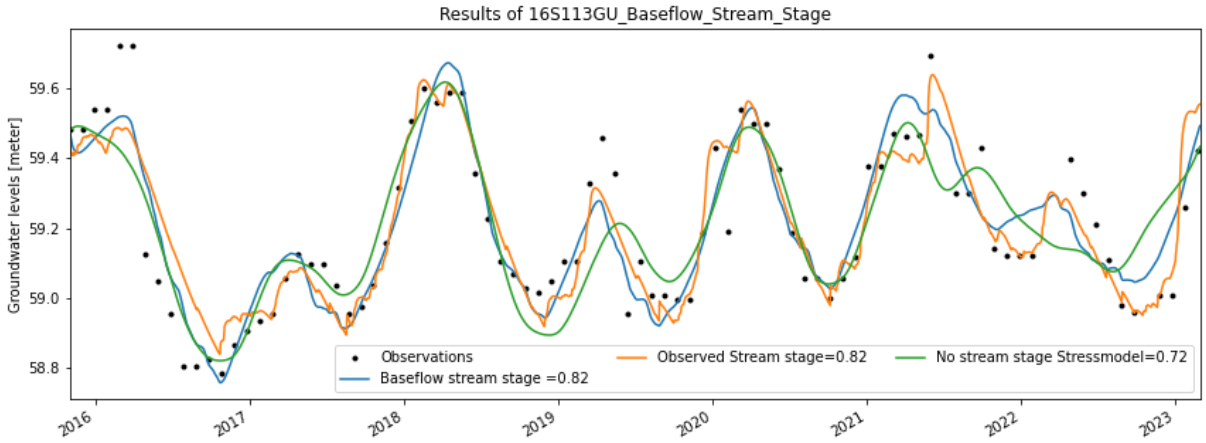

Figure 23 - Results of Model 15GW calibration on data from well 15S113GU.

The three time series models fitted to well 15S113GU showed varying results with coefficients of determination, R^2, ranging from 0.72 to 0. R^2=0.82 indicates that of the varying model outputs, 84% have been explained by predicting the outcome using the model.

Looking at figure 23 the results when using the observed stream stage indicate a good fit with the calibration time series. It follows both the highs and the lows of the observations. Using baseflow values for the stream stage stress model results in a similar result regarding R^2, AIC and RMSE as the observed stream stage, see appendix G. It does however result in smoother groundwater fluctuations with less quick changes. This is more in line with what is expected as this aquifer indicates slow changes throughout the observation period. Disregarding stream stage as a stress

model entirely results in a worse result than applying in looking at all parameters and it is thus disregarded for further analysis. For application the AIC, the RMSE and the R^2 were evaluated along with the validation plot found in figure 24. The validation in figure 24 was done against data collected manually once every month. In the figure its seen that the model using observed stream stage expects a groundwater rise way beyond what has been seen previous years whilst the model with baseflow stream stage expects a rise similar to that of previous years. Due to this the model using baseflow stream stage is continued to application.

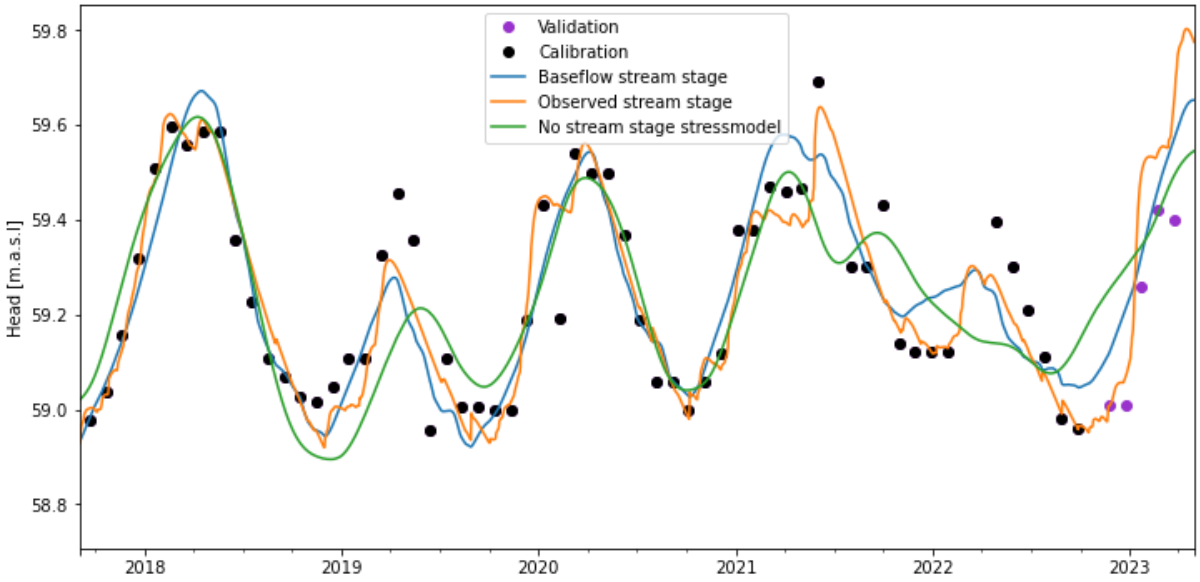

Figure 24 - Validation of Model 15GL.

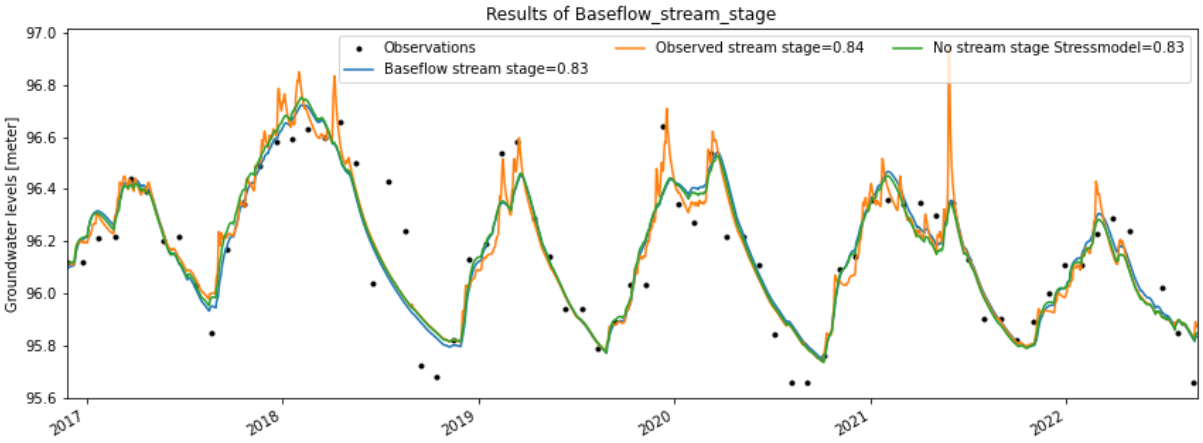

Figure 25 - Results of Model 16WL calibration on data from well 16S113GU

The same calibration was done for well 16S113GU, the result of that calibration is presented in figure 25. The calibration indicates similar results for all of the three models. The coefficient of determination is similar for each model and so are the values of AIC and RMSE, see appendix H. The calibration plot found in figure 25 is also present very similar results. The observed stream stage is the most different of the three exhibiting relatively large, quick changes in groundwater head. Evaluating the validation plot in figure 26 its clear that the observed stream stage model is the best for application as in the figure it is the only model following the pattern of groundwater fluctuation observed by the pressure transducers.

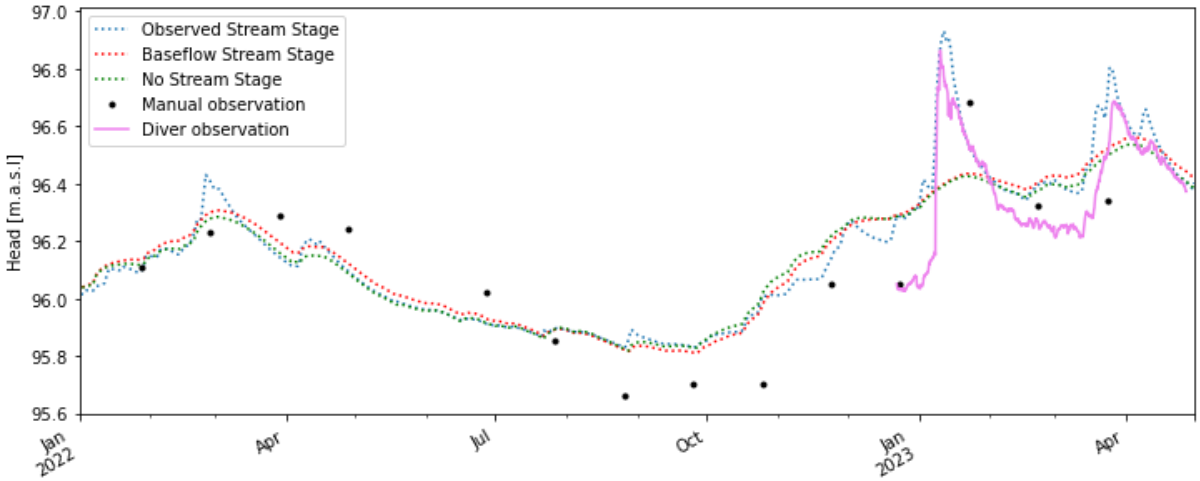

Figure 26 - Validation of Model 16WL.

From the modelling results the important stresses for each of the chosen models were evaluated. In figure 28 contributions to the model result from the different stresses are displayed. In figure 28, its seen that Model 15GW, calibrated on observations in a well connected to the same aquifer as 22S107GU and 22S108GU which had very poor correlations to stream head, does not take much input from the baseflow time series which resulted in only diffuse recharge being selected as a stress. As the data observations indicate that no quick connection exists between the two waterbodies this is deemed a likely result. For Model 16WL, connected to a well with high correlation to the stream stage the stress applied by the stream stage is more significant and has a clear impact on the model result. This can also be seen where the higher stream stage has a clear impact on the result of the model in figure 28. Observed stream stage settings makes the model follow the peaks much more accurately than the Baseflow settings which most likely has to do with that the impact of the input of observed stream stage follows a less monotone pattern which results in it having a larger impact on the model calibration than the baseflow stream stage would have.

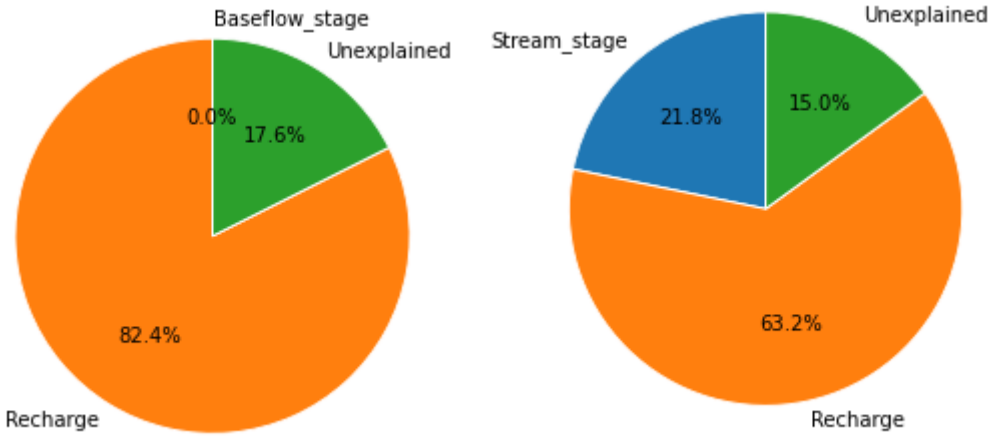

Figure 27 - Presenting the contribution of each stress model to the groundwater model result. Model 15GW on the left and Model 16WL on the right.

4.7 Groundwater level forecast

Changing the precipitation from 2022-10 and onwards to represent the different leakage scenarios and recalibrating the model resulted in the modelled results presented in figure 28 and 29. For Model 15GW the baseflow stream stage settings are used and for Model 16WL observed stream

stage was used. The leakage scenarios being 30 $\frac{l}{min*100m}$, 70 $\frac{l}{min*100m}$ and no leakage, in the figure described called Actual Recharge.

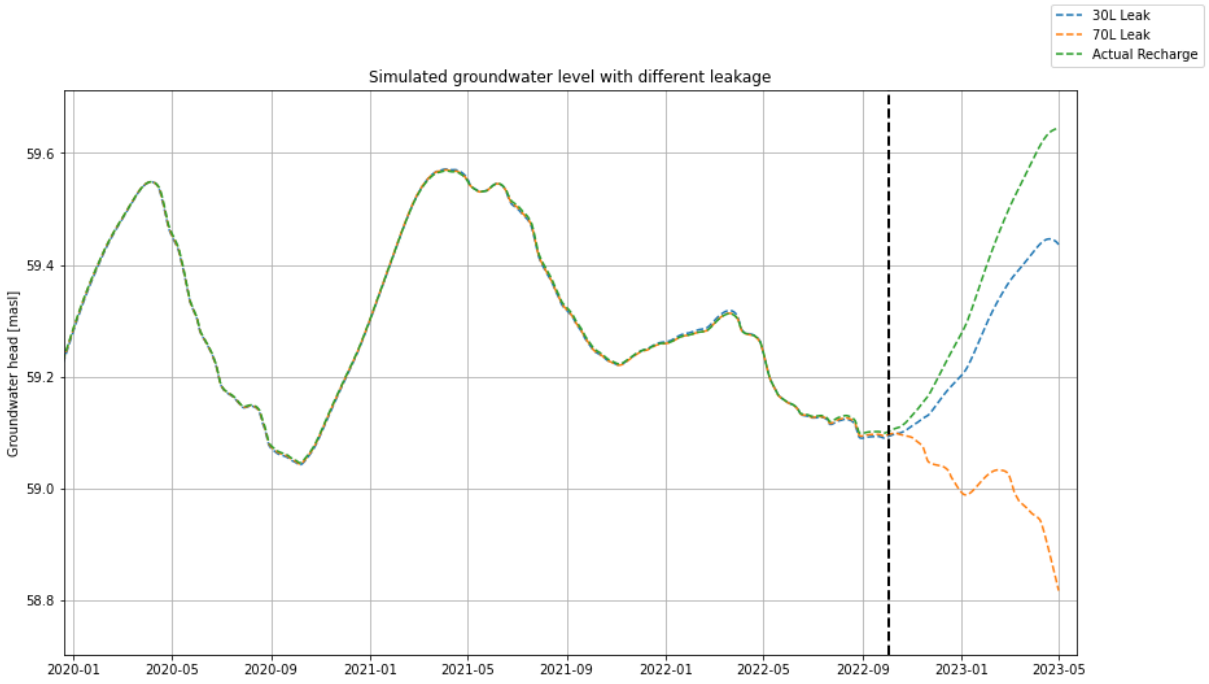

Figure 28 - Presenting the results from Model 15GL of different recharges in the glaciofluvial aquifer. Dashed line indicates when recharge starts to differ

In figure 30 the consequence of the leakage is clearly presented as a decrease in groundwater head. Actual recharge is forecasted to rise to the levels a little higher than previous years which is reasonable as according to *SMHI* the precipitation in the area the last 6 months have been more plentiful than an average year. At a leakage rate of 30 liters per minute and 100 meters a significant recharge of the aquifer is still expected. However, below that the aquifer clearly does not reach the expected head level looking at previous years. At the max leakage investigated no head increase occurs at all and the groundwater aquifer is simply decreasing throughout the period of the year where it would be expected to increase significantly.

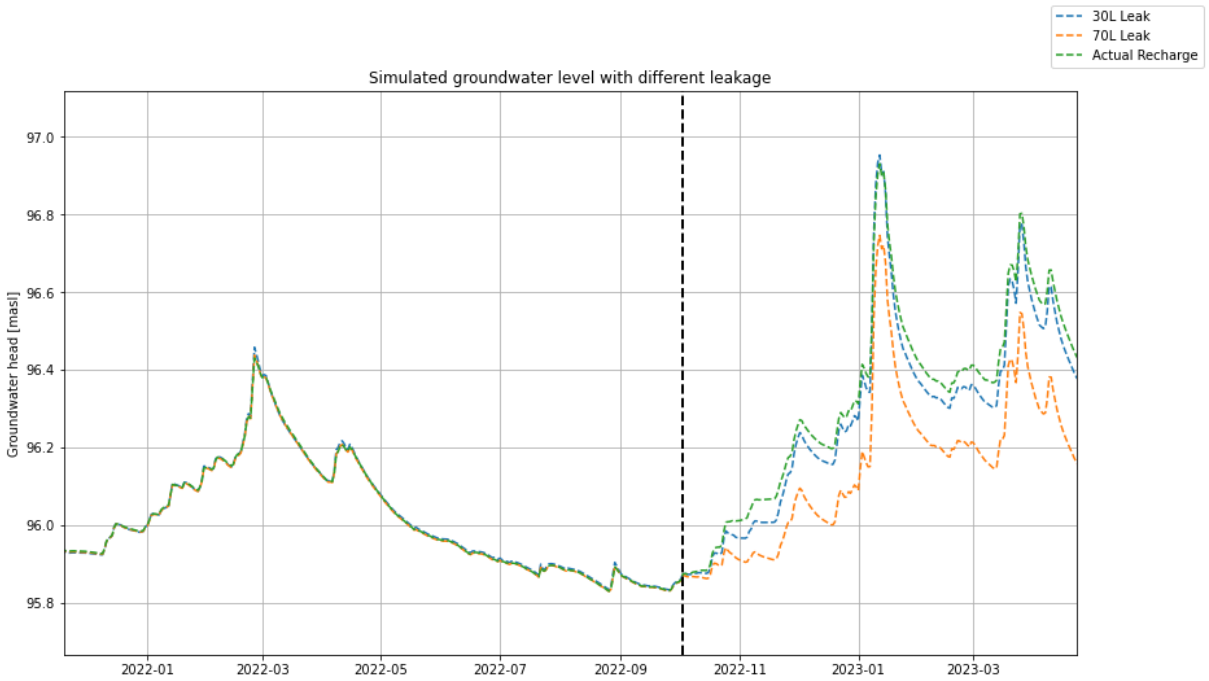

Figure 29 - Presenting the results from Model 16WL of different recharges in the wetland aquifer. Dashed line indicates when recharge starts to differ.

Unlike for the model discussed previously the aquifer connected to well 16S113GU does not seem to be as sensitive to the decrease in recharge. In figure 29 it is clear that the groundwater heads decrease significantly but recharge still occurs during the highest leakage scenario. As the aquifer where well 15S113GU is placed receives less recharge, see the groundwater head increase in figure 19, it is reasonable that it shows a more drastic response to a lack of recharge than the aquifer where 16S113GU is located which seems to receive more recharge.

If recharge is affected to this extent, the area of *Getå* nature reserve may see some serious impact as a consequence of the tunnel construction. As reduced, or in the worst case, a completely removed recharge will negatively affect eventual groundwater wells, root zones and as the stream is groundwater fed it will affect the stream flow. Especially as the decrease has not stopped as of the end of the simulation. Figure 30 and 31 presents the difference in groundwater head between the leakage scenarios and the actual recharge. In it the drawdown has not stopped as the differences are continuously increasing over time. This indicates that the full consequence of the leakage may not be fully visible until early in the year after leakage begins. For Model 16WL there is not as clear of a trend of increased head difference over time as the head difference decreases during the period where quick changes occur. However, over the entirety of the modelled period an increase can be seen in the higher leakage scenario whilst the smaller leakage scenario indicates that a relative steady state has been reached.

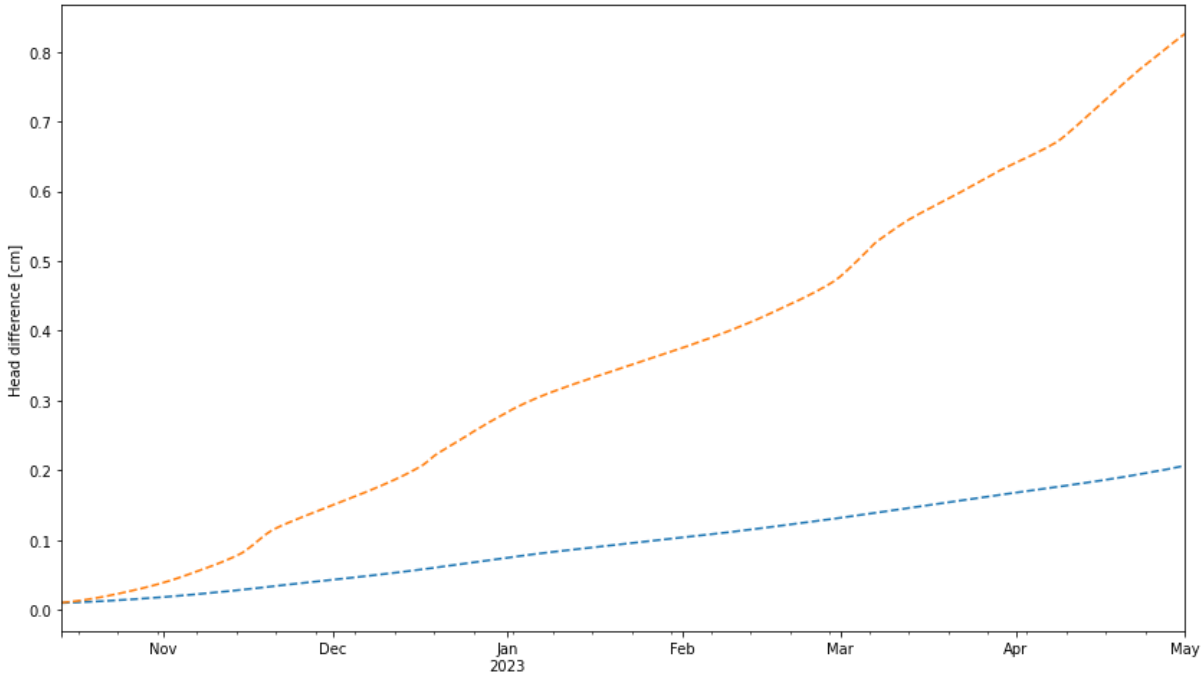

Figure 30 - Head difference between actual recharge and the leakage scenarios for Model 15GW

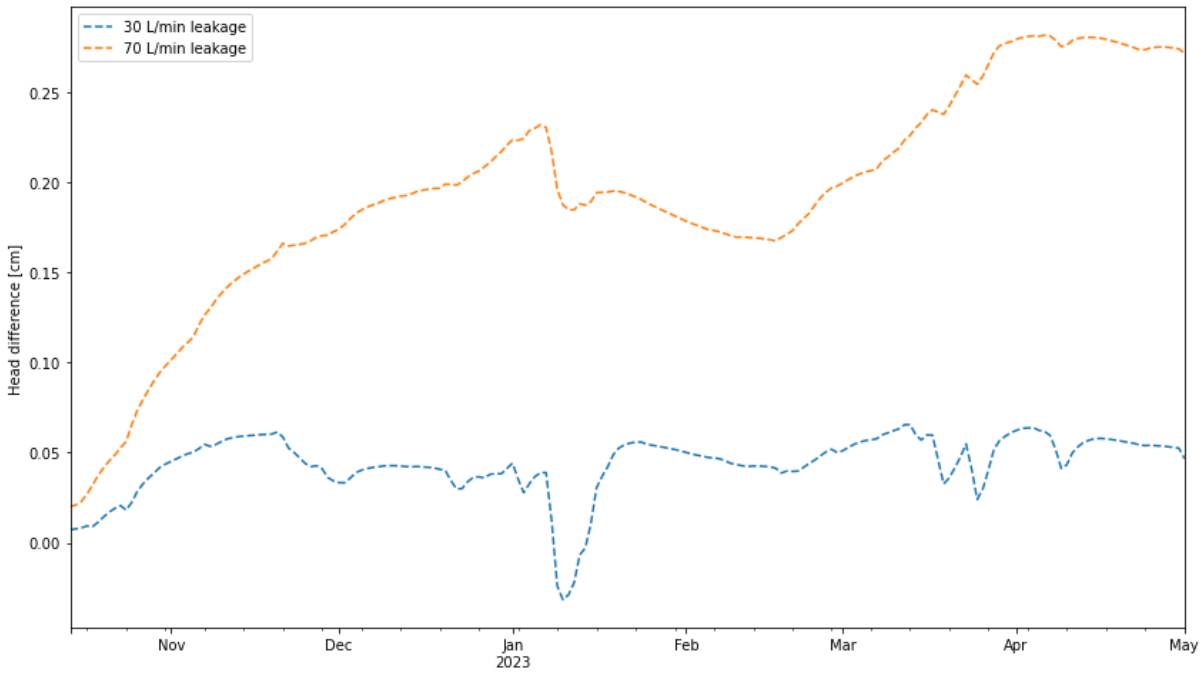

Figure 31 - Head difference between actual recharge and the leakage scenarios for Model 16WL

While this clearly indicates the long-term consequences of the tunnel construction it also establishes that there is time during construction to apply measures to the leakage before the it becomes unsustainable. The difference between the model results also clearly indicates that whilst the area is responding to recharge events simultaneously the response is different depending on the aquifer evaluated. Even within the area of *Getå* the fluctuations of groundwater head differ significantly. When applying time series modelling the model needs to be validated at the specific site to ensure that the result is applicable.

5. Discussion

The models made in this project can further be compared to other time series models from other projects. Finding this specific example of leakage application isn't simple but the model result can be compared to other hydrogeological time series models by evaluating the Nash-Sutcliffe Efficiency, NSE. This project has only calculated NSE of the model based on well 16S113GU as well 15S113GU doesn't have a validation time series allowing it. Model 16WL has an NSE of 0.46. Compared to other hydrogeological time series models this value is relatively low. Compared to the models trialed in [45] which reach an NSE of around 0.8 and in [57] where the models reach 0.84, 0.86 and 0.58. The models in these reports have longer and more accurate calibration time series which could explain the variation in results.

However, even with an improved calibration time series there are other improvements tied to this project which could be made. Such as further improving the evaporation model and confirming the conceptualization of the site. Throughout the project the assumption has been that the creek is gaining from the groundwater in nearby groundwater wells and evaluations done strengthen this assumption. They are however not enough to undoubtedly confirm the conceptual model. An improved understanding of the conceptual model may also allow for further input of stress models for stresses unidentified in this project resulting in further improvement.

Important to keep in mind when running the different calibrations is that the assumption of everything being the same when using baseflow stream stage or observed stream stage may not be true. In reality the baseflow of *Getåbäcken* would correspond to another set of groundwater observations than those that have been applied in calibration in this report. Furthermore, given that baseflow is considered dry-weather-flow its application in the model without adjusting the recharge model to correctly represent the conditions where baseflow is naturally found creates a model of a not entirely realistic scenario. If continued work aims to use the model for more detailed application and as a basis for decision making this may need to be addressed via further conceptualization of the site and improved detail when creating the model.

5.1 Precipitation storage in snow

An important part of the water cycle in subzero environments is storage of precipitation in the forms of snow and ice. Addition of snow storage to the model is simple to do in *Pastas* if FlexModel is the recharge model used. It can, as of yet, only be applied when using FlexModel and, if applied, snow storage is considered according to the Degree-Day-Based snow model detailed in *Model smoothing strategies to remove microscale discontinuities and spurious secondary optima in objective functions in hydrological calibration* [58].

However, as the case study area has varying positive and negative temperatures throughout winter no major snowmelt occurs as there would in an area with consistent negative temperatures throughout winter. Furthermore, as the baseflow analysis show flow increases throughout winter and data of snow layer depth from the closest *SMHI* station shows that throughout the winter the snow layer fluctuates in thickness [59] it is assumed that snowmelt occurs throughout winter and not all at once in spring. As applying snow storage to Model 15GW and Model 16WL mainly brings more uncertainties and less accuracy along with the data indicating that snow storage is not a major factor in *Getå* Nature Reserve this project does not take snow storage into account in the recharge models.

5.2 Uncertainties

None of the models forecast a situation perfectly in line with the observations used for validation. As models are never exact representations of reality this isn't surprising. However, uncertainties may be

amplified by observation data handling. In figure 32 the diver data and the manual observations which the models are calibrated on are displayed.

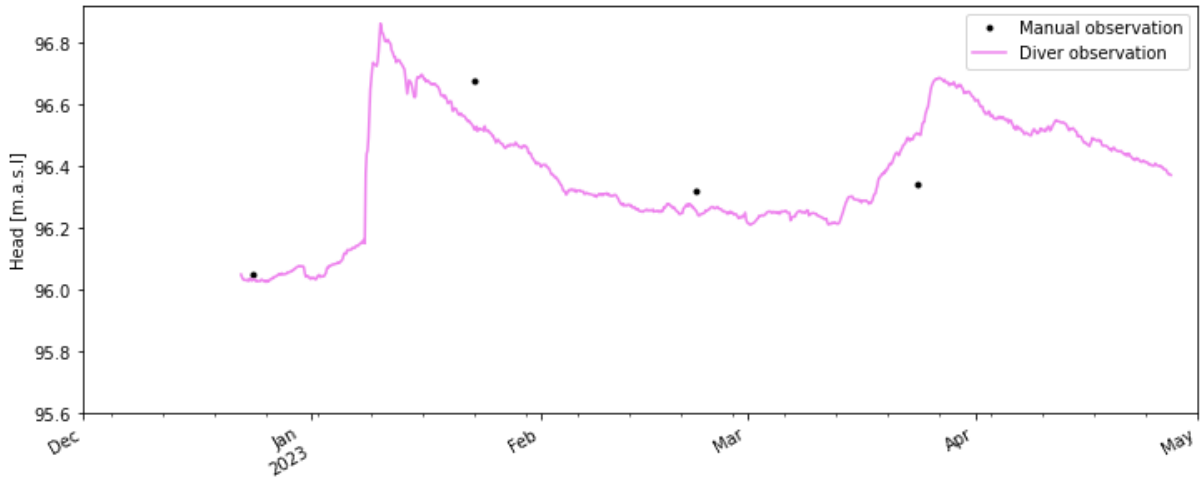

Figure 32 - Comparison of manual and diver observations

The figure shows that the measurements carried out manually with a dipper do not match those collected with the automatic pressure transducer. The assumption is that this would simply have to do with miscalculations in the diver data transformation from water above the diver to m.a.s.l. However, given that the manual observations are not consistently below or above the diver data an error in manual data collection may be the issue. As the model calibrates on these datasets uncertainties as a result of this is applied into the model.

Furthermore, as the model is in part based on the modelled S-HYPE flow uncertainty tied to that model is adopted into this project. *SMHI* apply the S-HYPE model, which, being a model, is not a perfect representation of reality. One situation where errors in the HYPE model may affect this project is the highest peaks visible in figure 20. The peak affecting the calibration of this project visible in 2021 has no clear basis in the other meteorological parameters in the area. No major rain or snowmelt occurred but even, so HYPE presents a major peak which affects the stream stage stress model.. The assumption is that none of these uncertainties affect the result of the groundwater model to a large extent, but they help explain some of the errors the model may present in its result.

Further uncertainties are tied to the application of leakage in the modelling process. A removal of precipitation assumes linear affect of leakage throughout the area. This is of course not the case. The leakages will result in local drawdown which will spread outward creating a cone of depression in the groundwater surface. As the size, depth and specific location of this cone is unknown it is not possible to state how exactly the area will react. It may be that the result of this project is accurate but it may also end up being irrelevant as reality is not governed by an equal, non-geographical, drawdown. During the project attempts were made to conceptualize the leakage as pumping wells. This however was dropped in favor of the decrease in precipitation as the information of leakage amount, location and rate were difficult to accurately estimate.

Furthermore, using precipitation as the leakage simulation along with FlexModel creates a situation where the recharge is further decreased beyond what the only the leakages would result in. This is due to the conceptualized interception basin requiring a specific volume of water before it allows for further percolation. Given that a decrease in recharge by increasing evaporation also affects the interception basin a string of wells may be the most accurate way to model an elongated leakage

point as a tunnel would represent. However, with the difficulties stated before associated to this concept this project did not further attempt it.

5.3 Continued research and future studies

To improve on this work further observations should be completed in the area. Creating a longer, high frequency dataset which can cover seasonal changes and allow for observations of quick groundwater head changes can achieve a more complete picture of the future groundwater head. Figure 33 shows the calibration of Model 16WL on the diver data. This calibration achieves an RMSE of 0.05 and an R^2-value of 94.05, a significantly better fit than the model calibrated on monthly values. However, as this dataset is not long enough to alleviate uncertainties application of this model is unsuitable. It does however indicate that with high frequency datasets model results may be significantly improved. The fit report for this calibration is found in appendix J.

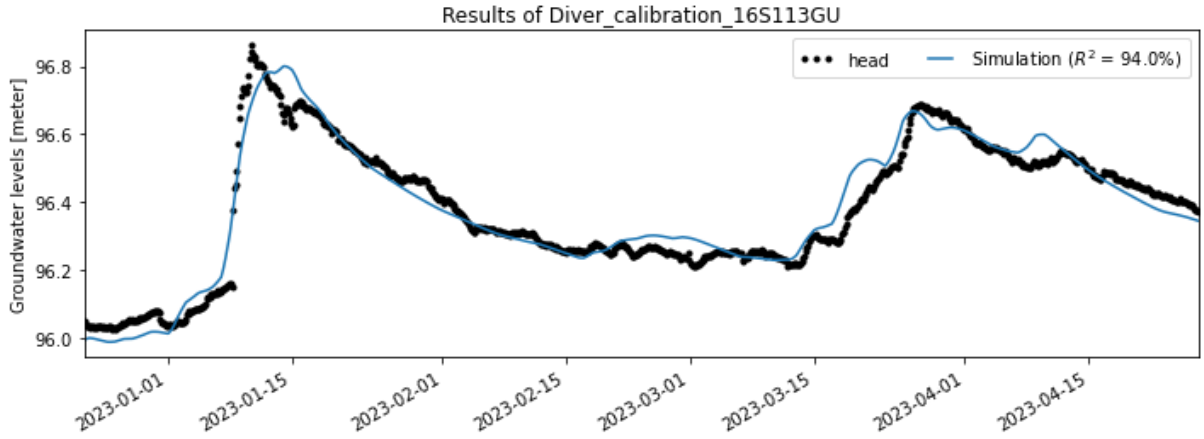

Figure 33 - Result of model calibrated on diver observations.

To tie the groundwater head change to the flow in the creek the tracer tests should also be continued to create a more solid dataset. This would allow for the planned interpolation of a trendline in the dataset which can, with more certainty, describe the relationship between groundwater fluctuations and stream flow variations.

As hydrological systems are highly dependent on seasonality a dataset that covers this needs to exist to ensure successful calibration. In places where such datasets do not exist prior to modelling initiation it may be more applicable to use other modelling methods. Further research should therefore include studies in to whether sites with similar parameters can borrow time series data from each other. In other words, could the time series from *Getå* nature reserve be applied in modelling in an area which is geographically different from *Getå* but hydrogeologically similar? Research in to this topic is underway, see [60], more time and input in to this area of study could help unlock the full range of applications for time series analysis and help bypass the need for local data sets.

Time series analysis applications should also be done in areas where the situation is dissimilar to that of *Getå* Nature Reserve. How does time series modelling and Pastas specifically function in an area where snowmelt fills a bigger role? Would the uncertainties found when applying snow in this project remain? Time series modelling has been successfully applied evaluate artificial infiltration [46] and in this project to evaluate the change in surface water head, both projects do evaluations because of tunnel leakage. Further applications of time series modelling within the field of hydrogeology could be found.

6. Conclusions

The responses to recharge in *Getå* Nature reserve can be observed to occur simultaneously throughout the area in multiple underground aquifers as well as the surface waterway *Getåbäcken*. Hydrogeological connections between the flow in *Getåbäcken* and nearby groundwater aquifers are hinted at by the baseflow separation analysis, the correlation analysis made between the baseflow as well as the groundwater head fluctuations observed.

Applying the groundwater head model to evaluate leakage scenarios indicate that leakages into the East Link tunnel will result in significant drawdown in aquifers where the tunnel traverses. It also hints that the glaciofluvial aquifers in center of the catchment area is more sensitive to recharge loss than the glaciofluvial aquifer located in the west of the catchment area. A leakage rate of 30 $\frac{l}{min*100m}$ results in groundwater drawdown in both evaluated aquifers, whilst a leakage of 70 $\frac{l}{min*100m}$ makes the aquifer in the areas center suffer a complete loss of recharge. The aquifer to the west simply suffers additional drawdown. It is also shown that the drawdown has not finished at the end of the simulation. Further drawdown is expected as a result of the leakages before a new steady state is achieved.

As the connections between groundwater aquifers and stream flow are clear measures should be taken to limit the leakages in to the tunnel as quickly as possible. The area exhibit quick responses to recharge stresses and the geology allows for quick groundwater flows. From the modelling there is a time of respite before the drawdown reaches problematic levels in both leakage scenarios. Before this time is up measures should have been taken, otherwise the East Link project runs a significant risk of lowering the flow in *Getåbäcken* due to groundwater drainage.

References

[1] H. M. Valett and A. M. Reinhold, “Groundwater and Surface Water Interaction,” *Encyclopedia of Inland Waters (Second Edition),* pp. 348-362, 2022.

[2] J. C. Sundby and E. K. Archer, “Hver dag brukes 193.000 liter drikkevann for at hur ikke skal synke,” *NRK,* 16 06 2022.

[3] F. Mossmark, “Groundwater Chemistry affected by Underground Construction Activities,” Göteborg, 2010.

[4] J. Kværner and P. Snilsberg, “Hydrogeological impacts of a railway tunnel in fractured Precambrian gneiss rocks (south-eastern Norway).,” *Hydrogeol J,* vol. 21, p. 1633–1653, 2013.

[5] G. Sällfors, Geoteknik - Jordmateriallära - Jordmekanik, Göteborg: Cremona, 2013.

[6] X. Chen, W. Dong, G. Ou, Z. Wang and C. Liu, “Gaining and losing stream reaches have opposite hydraulic conductivity distribution patterns,” *Hydrology and Earth System Sciences,* pp. 2569-2579, 2013.

[7] T. C. Winter, H. W. Judson, F. O. Lehn och W. M. Alley, ”Groundwater and Surface Water, A Single Resource,” US. Geological Survey, Denver, Colorado, 1998.

[8] J. Harding, E. Benfield, P. Bolstad, G. Helfman and E. Jones, “Stream Biodiversity: The ghost of land use past,” *PNAS,* vol. 95, 1998.

[9] Swedish Environmental Protection Agency, “Våtmarker och Klimat,” [Online]. Available: https://www.naturvardsverket.se/amnesomraden/vatmark/vatmarker-och-klimat/. [Accessed 11 04 2023].

[10] N. Barton and E. Quadros, “Understanding the need for pre-injection from permeability measurements: What is the connection?,” *Rock Mechanics and Geotechnical Engineering,* vol. 11, no. 3, pp. 576-597, 2019.

[11] M. P. Anderson, W. W. Woessner and R. J. Hunt, “Applied Groundwater Modelling - Simulation of Flow and Advcective Transport,” 2015.

[12] K. Hipel and A. McLeod, Time Series Modelling of Water Resources and Environmental systems, Amsterdam: Elsevier, 1994.

[13] R. Collenteur, M. Bakker, S. Klop and F. Shaars, “Pastas: open source software for analysis of groundwater time series,” *Groundwater,* vol. 57, no. 6, pp. 877-885, 2019.

[14] Swedish Transport Administration, “The West Link Project,” 2023. [Online]. Available: https://bransch.trafikverket.se/en/startpage/projects/Railway-construction-projects/The-West-Link-ProjectVastlanken/. [Accessed 12 04 2023].

[15] Google Maps, *Getå Naturreservat, Getå Gunnarstorp, Åby.*

[16] SGU, *Kartvisaren - Jordarter 1:25000-1:100000,* 2023.

[17] SGU, *Kartvisaren - Berggrund 1:50000-1:250000,* 2023.

[18] Länsstyrelsen, "Getåravinen Naturreservat," [Online]. Available: https://www.lansstyrelsen.se/ostergotland/besoksmal/naturreservat/getaravinen-naturreservat.html?sv.target=12.382c024b1800285d5863a8b8&sv.12.382c024b1800285d5863a8b8.route=/&searchString=&counties=&municipalities=&reserveTypes=&natureTypes=&accessibility=. [Accessed 12 04 2023].

[19] VISS, *Getåbäcken,* 2023.

[20] SMHI, *Modelldata per område - område 4708,* 2023.

[21] Norrköpings Kommun, *Naturvårdsprogram 2008-2011,* 2008.

[22] E. Andersson, S. Cloth, A. Mitander, A. Nydahl, A. Quin, L. Selin and H. Styf, "PM miljökvalitetsnormer för vatten, Ostlänken delen Stavsjö-Loddby," Swedish Transport Administration, 2022.

[23] Ministry of Energy, Buissness and Industry, *Miljöbalk (1998:808),* 1998.

[24] SLU, *Geodata Extraction Tool,* 2023.

[25] SGU, *Kartvisaren - Jorddjup,* 2023.

[26] SMHI, *Nederbördsmängd (dygn),* 2023.

[27] SMHI, "Avdunstning," 2022. [Online]. Available: https://www.smhi.se/kunskapsbanken/hydrologi/vattnets-kretslopp/avdunstning-1.30720. [Accessed 12 04 2023].

[28] SMHI, *Vattenbalans,* 2023.

[29] SMHI, *Lufttemperatur (dygn),* 2023.

[30] G. Gonthier, "A Graphical Method for Estimation of Barometric Efficiency from Continuous Data - Concepts and Application to a Site in the Piedmont, Air Force Plant 6, Marietta, Georgia," Geological Survey (U.S.), 2007.

[31] Van Essen, "Diver-Office," 2023. [Online]. Available: https://www.vanessen.com/products/software/diver-office/.

[32] G. Sentlinger, *Introduction to Salt Dilution Gauging for Streamflow Measurement,* Fantom Scientific, 2015.

[33] R. Collenteur, M. Bakker, R. Calje and S. F, “Introduction,” 2023. [Online]. Available: https://pastas.readthedocs.io/en/latest/index.html. [Accessed 12 04 2023].

[34] F. R. Hall, “Base-flow Recessions - A Review,” *Water Resources Research,* vol. 4, no. 5, 1968.

[35] J. Xie, X. Lui, K. Wang, T. Yang, K. Liang and C. Liu, “Evaluation of typical methods for baseflow separation in the contigous United States,” *Journal of Hydrogeology,* vol. 583, 2020.

[36] xiejx5, *Baseflow,* 2023.

[37] J. K. Wouter, J. E. Freer and R. A. Woods, “Technical note: Inherent benchmark or not? Comparing Nash–Sutcliffe and Kling–Gupta efficiency scores,” *Hydrology and Earth System Sciences,* vol. 23, no. 10, 2019.

[38] M. Kittridge, ”Introduction,” 2018. [Online]. Available: https://eto.readthedocs.io/en/latest/intro.html. [Använd 06 05 2023].

[39] R. G. Allen, L. S. Pereira, D. Raes och M. Smith, ”Crop evapotranspiration - Guidelines for computing crop water requirements,” FAO - Food and Agriculture Organization of the United Nations, Rome, 1998.

[40] SMHI, *Relativ luftfuktighet (h),* 2023.

[41] SMHI, *Vindriktning och vindhastighet (h),* 2023.

[42] SMHI, *Globalstrålning,* 2023.

[43] SMHI, *Solskenstid (h),* 2023.

[44] R. A. Collenteur, ”Snow,” 2021. [Online]. Available: https://pastas.readthedocs.io/en/latest/examples/12_snowmodel.html.

[45] R. A. Collenteur, M. Bakker, G. Klammler och S. Birk, ”Estimation of groundwater recharge from groundwater levels using nonlinear transfer function noise models and comparison to lysimeter data,” *Hydrology and Earth System Sciences,* vol. 25, nr 5, pp. 2931-2949, 2021.

[46] A. Lindblom and L. Boström, *valuating transfer-function models to understand groundwater level impacts - A study of head changes due to drainage and infiltration in an underground infrastructure project.,* Gothenburg, 2021.

[47] W. Berendrecht, A. Heemink, F. van Geer and J. Gehrels, “A non-linear state space approach to model groundwater fluctuations,” *Advances in Water Resources,* vol. 29, no. 7, pp. 959-973, 2006.

[48] R. Collenteur, M. Bakker, R. Calje och Schaars., ”Response Functions,” 2023. [Online]. Available: https://pastas.readthedocs.io/en/v1.0.1/userguide/response_functions.html#Gamma-response-function.

[49] J. R. von Asmuth och M. F. Bierkens, ”Modeling irregularly spaced residual series as a continuous stochastic process,” *Water Resources Research,* vol. 41, nr 12, 2005.

[50] F. Boyd Enders, ”Britannica.com,” 2022. [Online]. Available: https://www.britannica.com/science/coefficient-of-determination.

[51] D. Christie och S. P. Neill, Comprehensive Renewable Energy, Elsevier, 2022.

[52] V. Profillidis och G. Botzoris, ”Chapter 6 - Trend Projection and Time Series Methods,” *Modeling of Transport Demand,* pp. 225-270, 2019.

[53] L. Li, H. Maier, D. Partington, M. Lambert och C. Simmons, ”Performance assessment and improvement of recursive digital baseflow filters for catchments with different physical characteristics and hydrological inputs,” *Environmental Modelling and Software,* vol. 54, 2014.

[54] P. R. Furey och V. K. Gupta, ”A physically based filter for separating base flow from streamflow time series,” *Water Resources Research,* vol. 37, pp. 2709-2722, 2001.

[55] W. Boughton, A hydrograph-based model for estimating the water yield of ungauged catchments, Newcastle, 1993, pp. 317-324.

[56] E. A. B. Eltahir och P. J.-F. Yeh, ”On the asymmetric response of aquifer water level to floods and droughts in Illinois,” *Water Resources Research,* vol. 35, nr 4, pp. 1199 - 1217, 1999.

[57] M. Lu, B. Rogiers, K. Beerten, M. Gedeon och M. Huysmans, ”Exploring river–aquifer interactions and hydrological system response using baseflow separation, impulse response modeling, and time series analysis in three temperate lowland catchments,” *Hydrology and Earth Systems,* vol. 26, pp. 3629-3649, 2022.

[58] D. Kavetski och G. Kuczera, ”Model smoothing strategies to remove microscale discontinuities and spurious secondary optima in objective functions in hydrological calibration,” *Water Resources Research,* vol. 43, nr 3, 2007.

[59] SMHI, ”Snödjup och markytans tillstånd (dygn): SMHIs stationsnät,” 2023. [Online]. Available: https://www.smhi.se/data/meteorologi/ladda-ner-meteorologiska-observationer#param=snowDepth,stations=core,stationid=86410.

[60] E. Haaf, M. Giese, T. Reimann och R. Barthel, ”Data-Driven Estimation of Groundwater Level Time-Series at Unmonitored Sites Using Comparative Regional Analysis,” *Water Resources Research,* vol. 59, nr 7, 12 06 2023.

Appendices

Appendix A – Baseflow separation code

```
import baseflow
import pandas as pd
import numpy as np
```

Importing relevant packages used to run the model.

```
path = f'{baseflow._path}/"Path_to_csv".csv' #Csv needs to contain date and flow in the same column separated by ","
Q, date = baseflow.load_streamflow(path)
```

Importing the dataset as well as using the extension to convert the data into the streamflow time series.

```
b, KGEs = baseflow.separation(Q, date, area=12356000) #Catchment area in m^2
print(f'Best Method: {b.dtype.names[KGEs.argmax()]}') #Extention calculates baseflow (b) and Kling Glupta Efficiency for each of the presented result columns
```

```
Best Method: EWMA
```

Extension runs on the dataset and presents the best method for baseflow separation based on the dataset. Printing the resulting parameters *b* and *KGEs* gives 12 different columns of data for *b* and a row of 12 elements for *KGE* which corresponds to each column. Highest KGE column is the baseflow used.

```
print(b)
```

```
[(0.04113545, 0.04113545, 0.045, 0.064, 0.04113545, 0.04113545, 0.04113545, 0.04113545, 0.04113545, 0.04113545, 0.04113545, 0.04113545)
 (0.04090623, 0.04090623, 0.045, 0.064, 0.04090623, 0.04110333, 0.04096115, 0.04117848, 0.04132994, 0.04117629, 0.0419096 , 0.04125642)
 (0.04044839, 0.04044839, 0.045, 0.064, 0.04044839, 0.04082393, 0.04059703, 0.04098558, 0.04119721, 0.04098168, 0.0425625 , 0.04109464)
 ...
 (0.031    , 0.031    , 0.031, 0.031, 0.031    , 0.02330257, 0.02300425, 0.02443084, 0.02407821, 0.02441736, 0.02854513, 0.02425353)
 (0.0321163 , 0.0321163 , 0.031, 0.031, 0.0321163 , 0.02269411, 0.02247337, 0.0238376 , 0.02336063, 0.02382475, 0.02863868, 0.02359651)
 (0.03215688, 0.03215688, 0.031, 0.031, 0.03215688, 0.02269877, 0.02300608, 0.02445694, 0.02279406, 0.02444321, 0.02925527, 0.02360915)]
```

```
print(KGEs)
```

```
[0.41756153 0.52256116 0.4848812  0.4547928  0.36706415 0.73831807
 0.72503793 0.77868952 0.76774866 0.77820167 0.78657718 0.77319896]
```

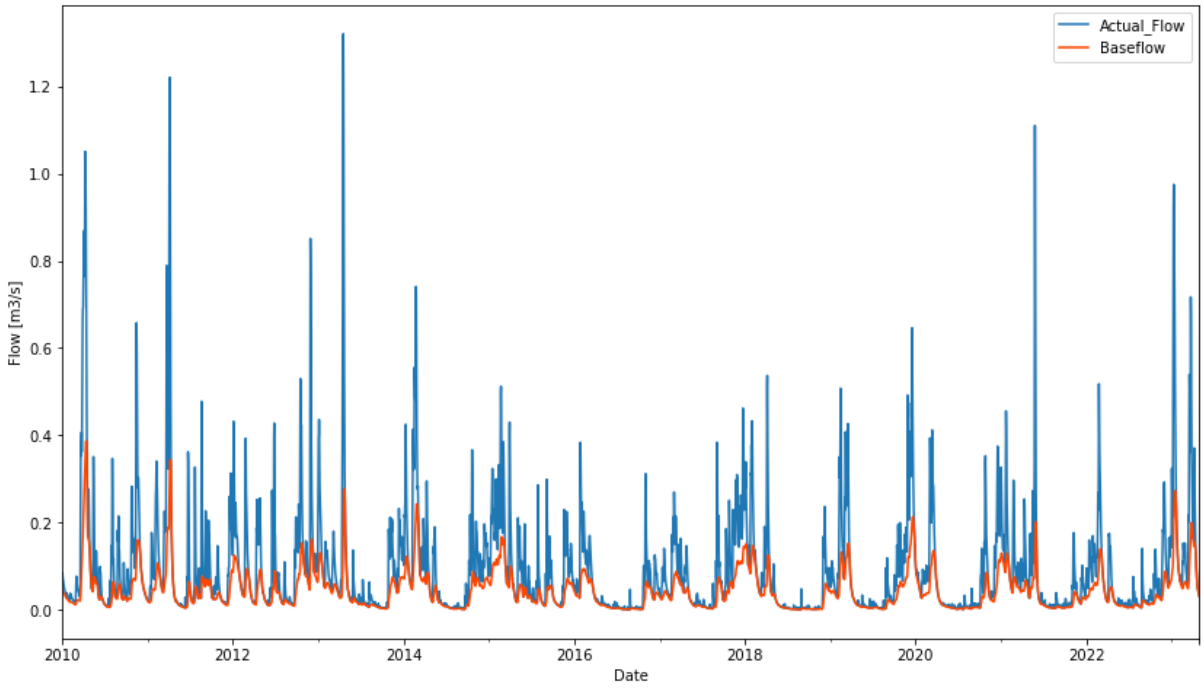

Figure 34 - Full baseflow time series plot

Appendix B – Evaporation model code.

Importing relevant packages used to run the model and export result into csv file.

```
import numpy as np
import pandas as pd
import matplotlib.pyplot as plt
import scipy.stats as stats
from numpy import savetxt
from eto import ETo, datasets
```

Cell reads the input file Eto.csv and prints the head of the table.

```
et1 = ETo()
tsdata = pd.read_csv("Eto.csv", sep=";", parse_dates=True, infer_datetime_format=True, index_col='date')
tsdata.head()
```

Cell with further input data, z_msl is meters above sea level, lat is latitude both referring to the station where data is collected. Freq indicates what frequency the model output is.

```
z_msl = 153.613
lat = 58.6892
freq = 'D'
```

This cell uses functions in the python extention to estimate other parameters needed than the once manually inputted.

```
et1.param_est(tsdata, freq, z_msl, lat)
et1.ts_param.head()
```

Executes the code with the estimated and inputted parameters to present the results.

```
eto1 = et1.eto_fao()
```

Appendix C – Groundwater model code

The groundwater model was, as mentioned, made with the Pastas extension, specifically version 1.01 which released during February of 2023. Certain aspects of the modelling were done before the update was live, but all parts of the code are ran on the 1.01 version. Pastas has a certain number of dependencies, other Python packages, that are required to run the extension. The aim of the modelling is as stated to create a model which can accurately model and predict groundwater changes in an area with input of sufficient quality. The only difference between the code for Model 15GW and Model 16WL is the groundwater dataset.

```
import matplotlib.pyplot as plt
import pandas as pd
import numpy as np
import pastas as ps
ps.show_versions()
```

```
Python version: 3.9.7
NumPy version: 1.20.3
Pandas version: 1.5.3
SciPy version: 1.10.1
Matplotlib version: 3.4.3
Numba version: 0.54.1
LMfit version: 1.1.0
Latexify version: Not Installed
Pastas version: 1.0.1
```

Import relevant packages and show the versions of the packages used.

```
#Preciptitaion data
precip = pd.read_csv("Precipitation_data.csv", sep=";", index_col="date", parse_dates=["date"],
                     ).squeeze().loc["2000":]
precip=ps.ts.pandas_equidistant_nearest(precip, "D") #Frequency is daily but the code sometimes has issues with the data anyway. This sets frequency daily.

#Groundwater Data
gwdata = pd.read_csv("Groundwater_data.csv", sep=";", index_col="date",  parse_dates=["date"],
                     ).squeeze().loc["2015":]
GWDATA=ps.ts.pandas_equidistant_nearest(gwdata, "30D") #Monthly frequency with inconsistant times between the measurements arent accepted by the model. Therefore 30 days are set as frequency.

#Evaporation data
evap=pd.read_csv("Evaporation_data.csv", sep=";", index_col="date", parse_dates=["date"],
                     ).squeeze()
evap=ps.ts.pandas_equidistant_nearest(evap, "D")
#Temperature data
Temp=pd.read_csv("Temperature_data.csv", sep=";", index_col="date", parse_dates=["date"],
                     ).squeeze()
Temp=ps.ts.pandas_equidistant_nearest(Temp, "D")
#Stream head data
Stream_head=pd.read_csv("Head_Getåbäcken_data.csv", sep=";", index_col="date", parse_dates=["date"],
                    ).squeeze()
```

Import datasets and determine frequencies.

```
#Noise model
n=ps.NoiseModel()

# Recharge Model
rch = ps.rch.FlexModel()
rm = ps.RechargeModel(precip, evap, recharge=rch, rfunc=ps.Gamma(), name="Recharge")

#Stress model connection to observed stream stage
w=ps.StressModel(Flow, rfunc=ps.Gamma(), name="Stream_stage", settings = "waterlevel")

#Stress model connection to baseflow stream stage
B=ps.StressModel(Baseflow, rfunc=ps.Gamma(), name="Baseflow", settings="waterlevel")

tmax="2022-09"
```

Running the model twice allows for further optimization. During the first calibration noise is not applied. This too increased the final optimization. Tmax simply indicates how long the calibration will run. If no value is presented it will end when the calibration series ends. Cells below are is the code used to apply stress models and run the model itself. For each of the three cells the only difference is the stressmodel pertaining to stream stage.

```
ml = ps.Model(GWDATA, name="Observed_Stream_stage")

ml.add_stressmodel(w)
ml.add_noisemodel(n)
ml.add_stressmodel(rm)
ml.set_parameter("Recharge_kv", vary=True)

ml.solve(
    noise=False, report=False, tmax=tmax
)
ml.solve(
    noise=True, initial=False, report=True, tmax=tmax
)
axes = ml.plots.results(figsize=(10, 6))
```

```
ml2 = ps.Model(GWDATA, name="Baseflow_stream_stage")

ml2.add_stressmodel(B)
ml2.add_noisemodel(n)
ml2.add_stressmodel(rm)
ml2.set_parameter("Recharge_kv", vary=True)

ml2.solve(
    noise=False, report=False, tmax=tmax
)
ml2.solve(
    noise=True, initial=False, report=True, tmax=tmax
)
axes = ml2.plots.results(figsize=(10, 6))
```

```
ml3 = ps.Model(GWDATA, name="No_stream_stage_stressmodel")

ml3.add_noisemodel(n)
ml3.add_stressmodel(rm)
ml3.set_parameter("Recharge_kv", vary=True)

ml3.solve(
    noise=False, report=False, tmax=tmax
)
ml3.solve(
    noise=True, initial=False, report=True, tmax=tmax
)
axes = ml3.plots.results(figsize=(10, 6))
```

Code for the plot seen in figure 23 and 24.

```
ax = ml2.plot(figsize=(12, 5))
ml.simulate().plot(ax=ax)
ml3.simulate().plot(ax=ax)
plt.legend(
    [
        "Observations",
        "Baseflow stream stage={:.2f}".format(ml2.stats.nse()),
        "Observed stream stage={:.2f}".format(ml.stats.nse()),
        "No stream stage Stressmodel={:.2f}".format(ml3.stats.nse()),
    ],
    ncol=3,
)
```

Code for plot seen in figure 25 and 26.

```
Diver=pd.read_csv("Head_16S113GU_202304.csv", sep=";", index_col="date", parse_dates=["date"], # Validation time series
                  ).squeeze()
a=ml.simulate(tmax="2023-05") #Simulation to end of validation time series for each model
b=ml2.simulate(tmax="2023-05")
c=ml3.simulate(tmax="2023-05")

plt.figure(figsize=(12,5)) #  Creating the plot, adding colors, linestyles and labels.
a.plot(label="Simulation", ls=":")
b.plot(label="Sim_Base", color="red", ls=":")
c.plot(label="No_flow", color="g", ls=":")
GWDATA.plot(label="Manual observation", color="black", style=".")
Diver.plot(label="Diver observation", color="violet", style="-")

plt.xlim("2022-12","2023-05") # Further information about the plot.
plt.xlabel("Date")
plt.ylabel("Head [m.a.s.l]")
plt.legend()
```

Application of models reads in new precipitation data.

```
precip_30 = pd.read_csv("precip_30.csv", sep=";", index_col="date", parse_dates=["date"],
                        ).squeeze().loc["2000":] # 30L
precip_30=ps.ts.pandas_equidistant_nearest(precip_30, "D")

precip_70 = pd.read_csv("precip_70.csv", sep=";", index_col="date", parse_dates=["date"],
                        ).squeeze().loc["2000":] # 30L
precip_70=ps.ts.pandas_equidistant_nearest(precip_70, "D")
```

Application creates new stressmodels and applies them to the same model as previously presented.

```
rchB_30 = ps.rch.FlexModel()
L30 = ps.RechargeModel(precip_30, evap, recharge=rchB_30, rfunc=ps.Gamma(), name="rch30")

rchB_70 = ps.rch.FlexModel()
L70 = ps.RechargeModel(precip_70, evap, recharge=rchB_70, rfunc=ps.Gamma(), name="rch70")
```

```
ml30 = ps.Model(GWDATA, name="30L_Leak")

ml30.add_stressmodel(L30)
ml30.add_noisemodel(n)
ml30.add_stressmodel(w)
ml30.set_parameter("rch30_kv", vary=True)

ml30.solve(
    noise=False, report=False, tmin="2015", tmax="2022-09"
)
ml30.solve(
    noise=True, initial=False, tmin="2015", tmax="2022-09", report=True,
)
```

```
ml70 = ps.Model(GWDATA, name="70L_Leak")

ml70.add_stressmodel(L70)
ml70.add_noisemodel(n)
ml70.add_stressmodel(w)
ml70.set_parameter("rch70_kv", vary=True)

ml70.solve(
    noise=False, report=False, tmin="2015", tmax="2022-09", initial=True
)  # First solve without noise model
ml70.solve(
    noise=True, initial=False, tmin="2015", tmax="2022-09", report=True,
)
```

Code for the plot in figures 27 and 28.

```
ax = ml.plot(figsize=(12, 6))
ax.set( ylabel='Groundwater head [masl]')
ml30.simulate().plot(ax=ax, ls="--")
ml70.simulate().plot(ax=ax, ls="--")
plt.legend(
    [
        "Observations",
        "Actual_Recharge ={:.2f}".format(ml.stats.nse()),
        "30L_Leak={:.2f}".format(ml30.stats.nse()),
        "70L_Leak={:.2f}".format(ml70.stats.nse()),
    ],
    ncol=3,
)
```

Code for the plot in figures 29 and 30.

```python
fig, ax = plt.subplots(figsize=(14,8))


ax.plot(Leak_30, label="30L Leak", ls="--")
ax.plot(Leak_70, label="70L Leak", ls="--")
ax.plot(Actual_Recharge, label="Actual Recharge", ls="--")

ax.set( ylabel='Groundwater head [masl]',
       title='Simulated groundwater level with different leakage')
ax.grid()

ax.axvline(19268, color="black", ls="--", linewidth=2)
ax.set_xlim(18950, 19470)
fig.legend()
plt.show()
```

```
Fit report 16S113GU_201611_202209         Fit Statistics
============================================================
nfev    57                      EVP                   77.20
nobs    63                      R2                     0.77
noise   True                    RMSE                   0.13
tmin    2016-11-25 00:00:00     AIC                 -239.48
tmax    2022-01-01 00:00:00     BIC                 -215.90
freq    D                       Obj                    0.50
warmup  3650 days 00:00:00      ___
solver  LeastSquares            Interp.                  No

Parameters (11 optimized)
============================================================
                   optimal    stderr      initial   vary
Stream_flow_A     0.190778  ±279.05%     0.221685   True
Stream_flow_n     0.353044   ±29.30%     0.368073   True
Stream_flow_a   791.447535  ±859.65%   792.379486   True
rch_A             8.168602  ±117.90%     6.501325   True
rch_n             1.772544   ±24.96%     1.852177   True
rch_a          1211.459338   ±11.75%  1152.243292   True
rch_fi            0.900000     ±nan%     0.900000  False
rch_fc            1.000000     ±nan%     1.000000  False
rch_sr            0.250000     ±nan%     0.250000  False
rch_de          211.413581  ±620.41%   155.403882   True
rch_l            22.562177  ±865.15%    14.998305   True
rch_m             0.500000     ±nan%     0.500000  False
rch_ks          233.341659  ±238.19%   154.884048   True
constant_d       73.940416   ±40.06%    73.614687   True
noise_alpha      20.429830   ±43.57%    30.000000   True

Warnings! (3)
============================================================
Parameter 'rch_m' on upper bound: 5.00e-01
Response tmax for 'Stream_flow' > than calibration period.
Response tmax for 'rch' > than calibration period.
```

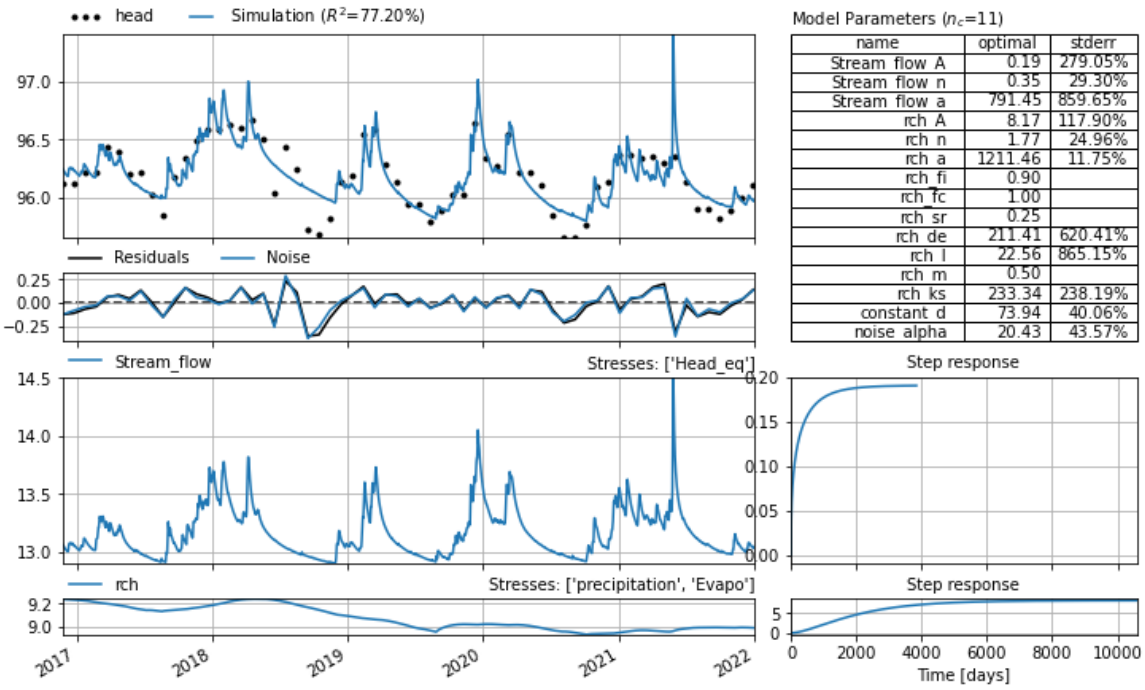

Model Parameters (n_c=11)

name	optimal	stderr
Stream_flow_A	0.19	279.05%
Stream_flow_n	0.35	29.30%
Stream_flow_a	791.45	859.65%
rch_A	8.17	117.90%
rch_n	1.77	24.96%
rch_a	1211.46	11.75%
rch_fi	0.90	
rch_fc	1.00	
rch_sr	0.25	
rch_de	211.41	620.41%
rch_l	22.56	865.15%
rch_m	0.50	
rch_ks	233.34	238.19%
constant_d	73.94	40.06%
noise_alpha	20.43	43.57%

Fit report presented by pastas showing the responses, stresses, results and the standard deviation of the different parameters. This only presents values as long as time series data of the calibration series is available. Further simulations can be done by using

```
ml.simulate(tmax="2023-04") # For any tmax as long as data for the stress models is avaliable.
```

This uses the optimized parameters to simulate the variable until tmax. Relevant results are only available as long as data for the stress models is available.

Appendix D – Tracer test results and dates

Table 7 - Results and dates of tracer tests

Date of test	Flow [l/s]
2023-04-27	137
2023-04-27	144
2023-03-06	73
2022-12-07	52
2022-12-07	64

Appendix E – Precipitation during observation period.

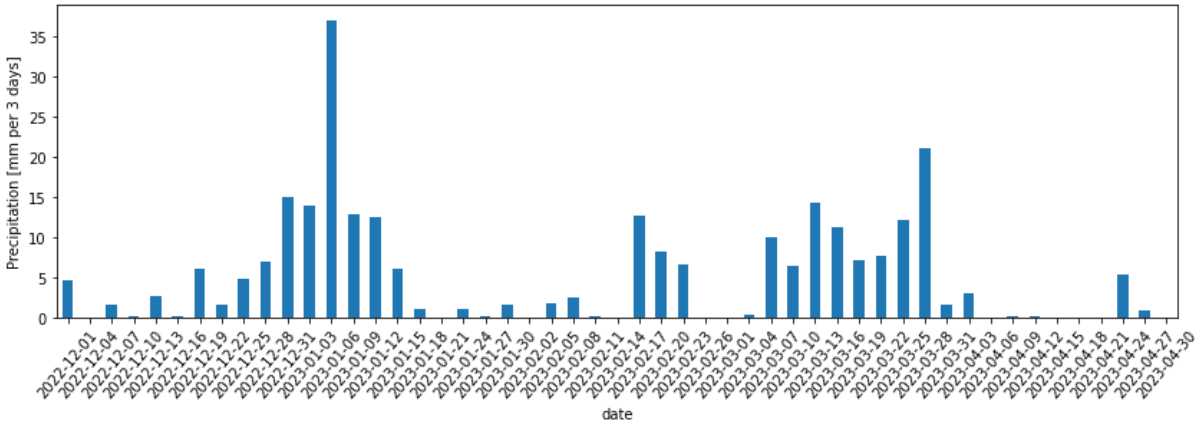

Figur 35 - Plot with precipitation in *Getå* Nature Reserve summed every 3 days for figure clarity.

Appendix F – Input time series' for model calibration

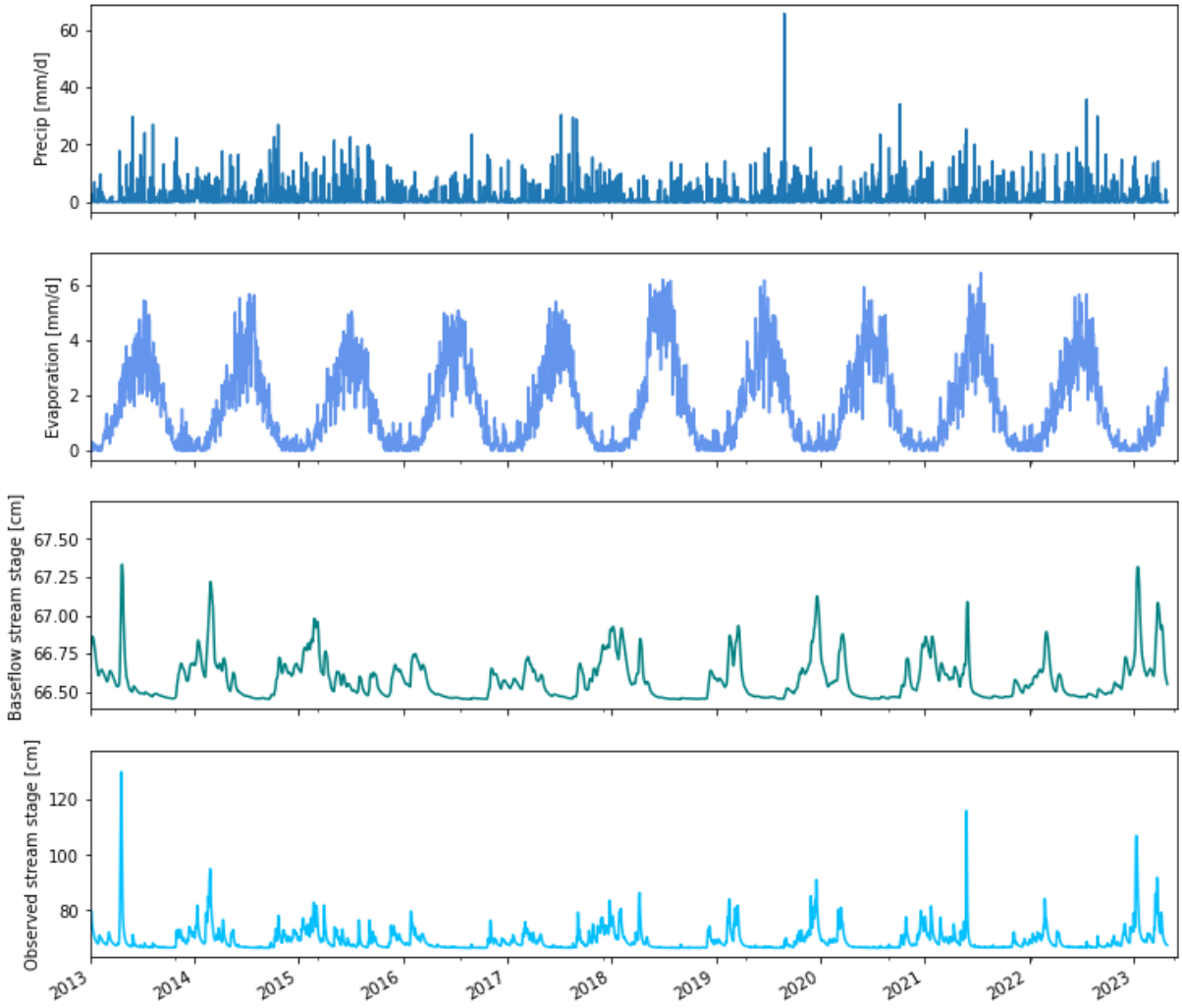

Figure 36 - Presents the input timeseries used in model calibration.

Appendix G – Calibration fit reports for Model 15GW

Fit report 15S113GU_Observed_Stream_Stage Fit Statistics

nfev	71	EVP	84.26
nobs	81	R2	0.84
noise	True	RMSE	0.09
tmin	2015-11-01 00:00:00	AIC	-374.61
tmax	2022-09-01 00:00:00	BIC	-345.88
freq	D	Obj	0.30
warmup	3650 days 00:00:00	___	
solver	LeastSquares	Interp.	No

Parameters (12 optimized)

	optimal	stderr	initial	vary
Stream_stage_A	0.261045	±33.11%	0.215504	True
Stream_stage_n	0.885619	±16.12%	0.825071	True
Stream_stage_a	305.520988	±44.74%	304.539736	True
Recharge_A	0.250137	±107.35%	0.330113	True
Recharge_n	4.202584	±110.53%	3.532972	True
Recharge_a	42.511846	±103.57%	57.922055	True
Recharge_srmax	941.892929	±2430.54%	947.366071	True
Recharge_lp	0.250000	±nan%	0.250000	False
Recharge_ks	91.391436	±3861.97%	98.980108	True
Recharge_gamma	0.763569	±1102.28%	0.682756	True
Recharge_kv	1.991048	±291.24%	0.919892	True
Recharge_simax	2.000000	±nan%	2.000000	False
constant_d	40.940380	±14.17%	43.961662	True
noise_alpha	34.114086	±30.30%	30.000000	True

Figure 38 - Fit report Observed stream stage Model 15GW.

Fit report 16S113GU_Baseflow_Stream_Stage Fit Statistics

nfev	30	EVP	83.57
nobs	81	R2	0.84
noise	True	RMSE	0.10
tmin	2015-11-01 00:00:00	AIC	-362.67
tmax	2022-09-01 00:00:00	BIC	-333.94
freq	D	Obj	0.34
warmup	3650 days 00:00:00	___	
solver	LeastSquares	Interp.	No

Parameters (12 optimized)

	optimal	stderr	initial	vary
Baseflow_stage_A	25.687854	±0.00%	26.153780	True
Baseflow_stage_n	66.709511	±0.00%	55.505145	True
Baseflow_stage_a	766.221885	±0.00%	248.232639	True
Recharge_A	2.783069	±19.44%	2.691247	True
Recharge_n	1.243438	±12.26%	1.287405	True
Recharge_a	180.221007	±21.76%	172.755029	True
Recharge_srmax	307.695222	±71.51%	296.461060	True
Recharge_lp	0.250000	±nan%	0.250000	False
Recharge_ks	1.512213	±22.35%	1.512500	True
Recharge_gamma	0.201424	±39.88%	0.191314	True
Recharge_kv	1.917845	±57.72%	1.907540	True
Recharge_simax	2.000000	±nan%	2.000000	False
constant_d	57.050588	±0.58%	57.094767	True
noise_alpha	24.154992	±33.53%	30.000000	True

Warnings! (1)

Response tmax for 'Baseflow_stage' > than calibration period.

Figure 37 - Fit report Baseflow stream stage Model 15GW.

Fit report 15S113GU_No_Stream_Stage Fit Statistics

nfev	25	EVP	79.30
nobs	81	R2	0.79
noise	True	RMSE	0.11
tmin	2015-11-01 00:00:00	AIC	-357.19
tmax	2022-09-01 00:00:00	BIC	-335.64
freq	D	Obj	0.39
warmup	3650 days 00:00:00	___	
solver	LeastSquares	Interp.	No

Parameters (9 optimized)

	optimal	stderr	initial	vary
Recharge_A	1.238043	±24.89%	1.142237	True
Recharge_n	1.543094	±15.34%	1.672268	True
Recharge_a	159.258713	±29.57%	136.996902	True
Recharge_srmax	209.309283	±231.27%	203.049433	True
Recharge_lp	0.250000	±nan%	0.250000	False
Recharge_ks	1475.406381	±1588.56%	1136.752247	True
Recharge_gamma	4.413450	±148.99%	4.102856	True
Recharge_kv	0.753468	±135.26%	0.736433	True
Recharge_simax	2.000000	±nan%	2.000000	False
constant_d	58.169943	±0.53%	58.219132	True
noise_alpha	32.849629	±30.71%	30.000000	True

Figure 39 - Fit report no stream stage Model 15GW.

```
Fit report 30L_Leak                    Fit Statistics
=====================================================
nfev     31                    EVP              83.59
nobs     81                    R2                0.84
noise    True                  RMSE              0.10
tmin     2015-11-01 00:00:00   AIC            -362.68
tmax     2022-09-01 00:00:00   BIC            -333.95
freq     D                     Obj               0.34
warmup   3650 days 00:00:00    ___
solver   LeastSquares          Interp.             No

Parameters (12 optimized)
=====================================================
                optimal   stderr      initial   vary
rch30_A        2.808111  ±18.69%     2.531856   True
rch30_n        1.260670  ±12.50%     1.353915   True
rch30_a      179.333375  ±21.11%   160.572163   True
rch30_srmax  288.109810  ±64.47%   280.102564   True
rch30_lp       0.250000     ±nan%     0.250000  False
rch30_ks       1.475268  ±22.25%     1.577194   True
rch30_gamma    0.191581  ±49.18%     0.203532   True
rch30_kv       1.923140  ±53.85%     1.964370   True
rch30_simax    2.000000     ±nan%     2.000000  False
Baseflow_A    15.697592   ±0.00%    21.401632   True
Baseflow_n    80.001473   ±0.00%    47.775670   True
Baseflow_a  6481.792234   ±0.00%   269.582931   True
constant_d    57.039383   ±0.57%    57.227755   True
noise_alpha   24.050511  ±33.16%    30.000000   True

Warnings! (1)
=====================================================
Response tmax for 'Baseflow' > than calibration period.
```

Figure 41 - Fit report 30 L leakage scenario Model 15GW.

```
Fit report 70L_Leak                    Fit Statistics
=====================================================
nfev     26                    EVP              83.57
nobs     81                    R2                0.84
noise    True                  RMSE              0.10
tmin     2015-11-01 00:00:00   AIC            -362.68
tmax     2022-09-01 00:00:00   BIC            -333.94
freq     D                     Obj               0.34
warmup   3650 days 00:00:00    ___
solver   LeastSquares          Interp.             No

Parameters (12 optimized)
=====================================================
                optimal   stderr      initial   vary
rch70_A        2.785505  ±20.90%     2.698385   True
rch70_n        1.249588  ±12.62%     1.288515   True
rch70_a      179.699855  ±21.86%   171.884734   True
rch70_srmax  301.575567  ±79.73%   315.448303   True
rch70_lp       0.250000     ±nan%     0.250000  False
rch70_ks       1.501450  ±21.43%     1.553070   True
rch70_gamma    0.198427  ±40.68%     0.203959   True
rch70_kv       1.922296  ±61.30%     1.999567   True
rch70_simax    2.000000     ±nan%     2.000000  False
Baseflow_A   116.739913   ±0.00%    96.897194   True
Baseflow_n    85.590014   ±0.00%    24.648737   True
Baseflow_a  9955.607071   ±0.00%  1121.414164   True
constant_d    57.051071   ±0.57%    57.113069   True
noise_alpha   24.302227  ±32.98%    30.000000   True

Warnings! (1)
=====================================================
Response tmax for 'Baseflow' > than calibration period.
```

Figure 40 - Fit report 70 L leakage scenario Model 15GW.

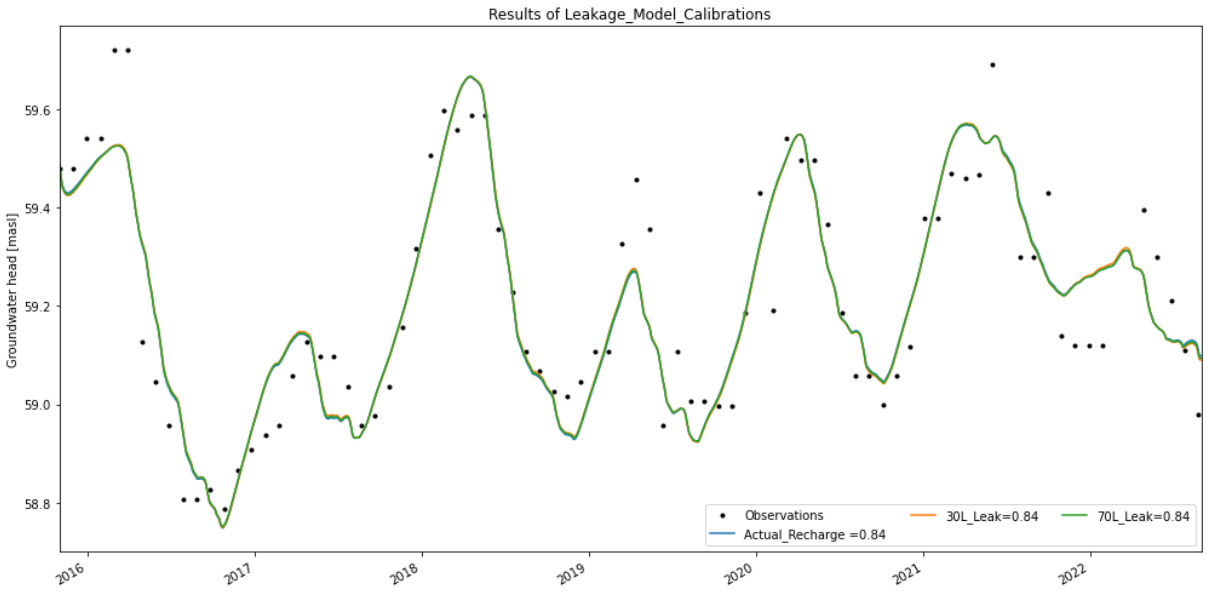

Figure 42 - Calibration of Model 15GW for the different leakage scenarios.

Appendix H – Calibration fit reports for Model 16WL

```
Fit report Observed_Stream_stage            Fit Statistics
============================================================
nfev    62                      EVP                  84.47
nobs    70                      R2                    0.84
noise   True                    RMSE                  0.11
tmin    2016-11-25 00:00:00     AIC                -291.57
tmax    2022-09-01 00:00:00     BIC                -264.59
freq    D                       Obj                   0.39
warmup  3650 days 00:00:00      ___
solver  LeastSquares            Interp.                 No

Parameters (12 optimized)
============================================================
                    optimal      stderr      initial   vary
Stream_stage_A     0.042827   ±370.29%     0.027078   True
Stream_stage_n     0.206815   ±103.66%     0.010021   True
Stream_stage_a   642.067572  ±1984.12%   258.157036   True
Recharge_A         3.575393   ±101.31%     3.443304   True
Recharge_n         0.608819    ±17.80%     0.799150   True
Recharge_a      1825.275151   ±130.32%  1574.128658   True
Recharge_srmax   131.256795    ±18.31%   141.679239   True
Recharge_lp        0.250000       ±nan%     0.250000  False
Recharge_ks        1.134292    ±32.00%     4.447950   True
Recharge_gamma     2.709739    ±59.10%     4.322267   True
Recharge_kv        0.536257    ±14.10%     0.486686   True
Recharge_simax     2.000000       ±nan%     2.000000  False
constant_d        91.157959    ±11.54%    91.311830   True
noise_alpha       12.521611    ±63.75%    30.000000   True

Warnings! (2)
============================================================
Response tmax for 'Stream_stage' > than calibration period.
Response tmax for 'Recharge' > than calibration period.
```

Figure 43 - Fit report Observed stream stage Model 16WL.

```
Fit report Baseflow_stream_stage            Fit Statistics
============================================================
nfev    90                      EVP                  82.68
nobs    70                      R2                    0.83
noise   True                    RMSE                  0.11
tmin    2016-11-25 00:00:00     AIC                -283.81
tmax    2022-09-01 00:00:00     BIC                -256.82
freq    D                       Obj                   0.43
warmup  3650 days 00:00:00      ___
solver  LeastSquares            Interp.                 No

Parameters (12 optimized)
============================================================
                    optimal      stderr      initial   vary
Baseflow_A         0.250712     ±0.00%     0.250712   True
Baseflow_n        49.342741     ±0.00%    51.363955   True
```

Figure 44 - Fit report Baseflow Stream Stage Model 16WL

```
Fit report No_stream_stage_stressmodel      Fit Statistics
============================================================
nfev    54                      EVP                  82.57
nobs    70                      R2                    0.83
noise   True                    RMSE                  0.11
tmin    2016-11-25 00:00:00     AIC                -289.47
tmax    2022-09-01 00:00:00     BIC                -269.23
freq    D                       Obj                   0.43
warmup  3650 days 00:00:00      ___
solver  LeastSquares            Interp.                 No

Parameters (9 optimized)
============================================================
                    optimal      stderr      initial   vary
Recharge_A         3.619433    ±87.02%     3.018132   True
Recharge_n         0.539082    ±12.41%     0.691112   True
Recharge_a      2119.235376   ±127.37%  1644.070926   True
Recharge_gamma     3.330463    ±37.71%     5.977955   True
Recharge_kv        0.546115     ±8.17%     0.513255   True
Recharge_simax     2.000000       ±nan%     2.000000  False
constant_d        94.058960     ±1.74%    93.680238   True
noise_alpha       12.485322    ±59.36%    30.000000   True

Warnings! (1)
```

Figure 45 - Fit report no stream stage Model 16WL.

```
Fit report 30L_Leak                          Fit Statistics
============================================================
nfev    63                    EVP                    84.75
nobs    70                    R2                      0.85
noise   True                  RMSE                    0.10
tmin    2016-11-25 00:00:00   AIC                  -292.73
tmax    2022-09-01 00:00:00   BIC                  -265.75
freq    D                     Obj                     0.38
warmup  3650 days 00:00:00    ___
solver  LeastSquares          Interp.                   No

Parameters (12 optimized)
============================================================
                     optimal      stderr       initial   vary
rch30_A             4.739291    ±59.66%      3.465503   True
rch30_n             0.635367    ±19.61%      0.796904   True
rch30_a          2353.978187    ±41.66%   1596.578014   True
rch30_srmax       130.817751    ±19.47%    142.918672   True
rch30_lp            0.250000        ±nan%      0.250000  False
rch30_ks            1.136899    ±28.64%      4.400492   True
rch30_gamma         2.618275    ±55.21%      4.267143   True
rch30_kv            0.531469    ±14.12%      0.487322   True
rch30_simax         2.000000        ±nan%      2.000000  False
Stream_stage_A      0.037199   ±435.11%      0.027385   True
Stream_stage_n      0.154155   ±125.22%      0.010074   True
Stream_stage_a    657.163100  ±3026.65%    488.030743   True
constant_d         90.881158    ±11.23%     91.274948   True
noise_alpha        11.762191    ±69.35%     30.000000   True

Warnings! (2)
============================================================
Response tmax for 'rch30' > than calibration period.
Response tmax for 'Stream_stage' > than calibration period.
```

Figure 47 - Fit report 30 L leakage scenario Model 16WL

```
Fit report 70L_Leak                          Fit Statistics
============================================================
nfev    34                    EVP                    84.58
nobs    70                    R2                      0.85
noise   True                  RMSE                    0.10
tmin    2016-11-25 00:00:00   AIC                  -292.01
tmax    2022-09-01 00:00:00   BIC                  -265.03
freq    D                     Obj                     0.38
warmup  3650 days 00:00:00    ___
solver  LeastSquares          Interp.                   No

Parameters (12 optimized)
============================================================
                     optimal      stderr       initial   vary
rch70_A             4.043982    ±90.31%      3.067163   True
rch70_n             0.621449    ±20.32%      0.611739   True
rch70_a          2074.841873    ±89.72%   1465.430539   True
rch70_srmax       130.846727    ±19.48%    132.096836   True
rch70_lp            0.250000        ±nan%      0.250000  False
rch70_ks            1.154967    ±25.09%      1.151170   True
rch70_gamma         2.687650    ±55.26%      2.886288   True
rch70_kv            0.533069    ±13.57%      0.539284   True
rch70_simax         2.000000        ±nan%      2.000000  False
Stream_stage_A      0.037085   ±350.20%      0.038647   True
Stream_stage_n      0.184137   ±108.31%      0.238630   True
Stream_stage_a    428.634233  ±2065.08%    248.869325   True
constant_d         91.258773     ±8.18%     91.747374   True
noise_alpha        12.384745    ±64.24%     30.000000   True

Warnings! (1)
============================================================
Response tmax for 'rch70' > than calibration period.
```

Figure 46 - Fit report 70 L leakage scenario Model 16WL.

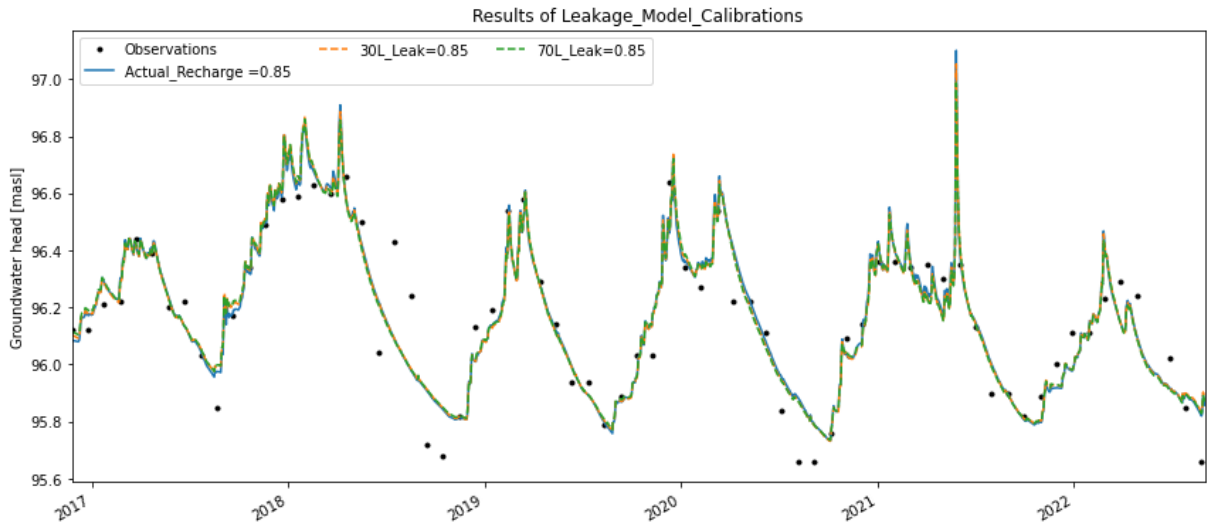

Figure 48 - Presenting the calibration of Model 16WL used to evaluate different leakage rates.

Appendix I – Calibration fit report for model calibrated on pressure transducer data

```
Fit report Diver_calibration_16S113GU        Fit Statistics
============================================================
nfev    199                     EVP                    94.09
nobs    1005                    R2                      0.94
noise   True                    RMSE                    0.05
tmin    2022-12-22 12:00:00     AIC                 -9343.42
tmax    2023-04-27 09:00:00     BIC                 -9284.46
freq    3H                      Obj                     0.04
warmup  3650 days 00:00:00      ___
solver  LeastSquares            Interp.                   No

Parameters (12 optimized)
============================================================
                    optimal      stderr      initial   vary
Stream_stage_A     0.059228   ±5451.16%     0.136164   True
Stream_stage_n     0.273863     ±31.51%     0.419045   True
Stream_stage_a  1177.509433  ±20046.31%  1109.317773   True
Recharge_A         4.802662   ±1936.05%     2.699367   True
Recharge_n         1.004646     ±48.17%     1.044083   True
Recharge_a       968.930033   ±1769.22%   823.360019   True
Recharge_srmax   204.907955    ±890.29%   115.339690   True
Recharge_lp        0.250000       ±nan%     0.250000  False
Recharge_ks       13.290728   ±1581.67%    20.675221   True
Recharge_gamma     1.836591    ±122.78%     1.587915   True
Recharge_kv        0.250000    ±337.17%     0.250013   True
Recharge_simax     2.000000       ±nan%     2.000000  False
constant_d        85.649980    ±132.60%    82.908549   True
noise_alpha        6.059786     ±37.52%     0.125000   True

Warnings! (3)
============================================================
Parameter 'Recharge_kv' on lower bound: 2.50e-01
Response tmax for 'Stream_stage' > than calibration period.
Response tmax for 'Recharge' > than calibration period.
```

Figure 49 - Fit report Model 16WL setting calibrated on transducer observations in well 16S113GU.